

**BRENER DE ALMEIDA OLIVEIRA**

**TIME SERIES INVESTIGATION FOR CORRELATIONS BETWEEN RAINFALL  
AND PHENOLOGY IN CERRADO (BRAZILIAN SAVANNA)**

Dissertation submitted to the Forest Science  
Graduate Program of the Universidade  
Federal de Viçosa in partial fulfillment of  
the requirements for the degree of *Magister  
Scientiae*.

Advisor: Cibele Hummel do Amaral

**VIÇOSA – MINAS GERAIS  
2020**

**Ficha catalográfica elaborada pela Biblioteca Central da Universidade  
Federal de Viçosa - Campus Viçosa**

T

Oliveira, Brener de Almeida, 1990-  
O48t Time series investigation for correlations between rainfall  
2020 and phenology in Cerrado (Brazilian savanna) / Brener de  
Almeida Oliveira. – Viçosa, MG, 2020.  
55 f. : il. (algumas color.) ; 29 cm.

Inclui apêndices.

Orientador: Cibele Hummel do Amaral.

Dissertação (mestrado) - Universidade Federal de Viçosa.

Referências bibliográficas: f. 49-55.

1. Fenologia. 2. Sensoriamento remoto. 3. Cerrados.  
4. Vegetação - Mapeamento - Índices. I. Universidade Federal de  
Viçosa. Departamento de Engenharia Florestal. Programa de  
Pós-Graduação em Ciência Florestal. II. Título.

CDO adapt. CDD 634.91811


**BRENER DE ALMEIDA OLIVEIRA**


**TIME SERIES INVESTIGATION FOR CORRELATIONS BETWEEN RAINFALL  
AND PHENOLOGY IN CERRADO (BRAZILIAN SAVANNA)**

Dissertation submitted to the Forest Science  
Graduate Program of the Universidade  
Federal de Viçosa in partial fulfillment of  
the requirements for the degree of *Magister  
Scientiae*.

APPROVED: February 19, 2020.

Assent:

  
Brener de Almeida Oliveira  
Author

  
Cibele Hummel do Amaral  
Advisor

## ACKNOWLEDGEMENTS

I thank God for my healthy life and for all the daily graces that sustain me. I thank the Federal University of Viçosa and the Forestry Department for the structure offered. I thank my dear advisor Cibele Hummel do Amaral, for all the partnership, understanding, and teachings, for having believed in my potential to develop this project. I thank the evaluating board for the availability and attention in evaluating my work. I thank my colleagues in the SIGMA laboratory for all the support and sharing of knowledge during these two years, especially Lucas Arthur de Almeida Telles, Nero Lemos Martins de Castro, Rodrigo Vieira Leite and Écio Souza Diniz for the companionship in all moments. I thank and dedicate this thesis to my family, father, mother, and sister, for all the love, attention, and affection they have to me.

This study was financed in part by the Coordenação de Aperfeiçoamento de Pessoal de Nível Superior – Brasil (CAPES) – Finance Code 001.

We also thank the National Council for Scientific and Technological Development (Conselho Nacional de Desenvolvimento Científico e Tecnológico - CNPq), for granting the scholarship.

## ABSTRACT

OLIVEIRA, Brener de Almeida, M.Sc., Universidade Federal de Viçosa, February, 2020. **Time-series investigation for correlations between rainfall and phenology in Cerrado (Brazilian savanna)**. Advisor: Cibele Hummel do Amaral.

The Brazilian savanna (Cerrado) is the second-largest biome in Brazil, following the Amazon. The influence of climate in this biome is pronounced, dry winters and rainy summers determines the characteristics of the Cerrado typologies. The effect of climate on vegetation can be assessed through the variation in biophysical responses of each Cerrado typology provided by time-series of spectral indices as Normalized Difference Vegetation Index (NDVI) and Enhanced Vegetation Index (EVI). This study aims to test for the correlation between rainfall and Cerrado typologies spectral responses from 2001 to 2018, in central Brazil. As specific objectives, we intend to spectrally separate such physiognomies and characterize them according to their phenological metrics. Thus, we performed a Principal Component Analysis (PCA) for the MOD13Q1 NDVI and EVI time-series, to test for the spectral separation of Cerrado typologies. We extracted the phenological metrics (e.g. growth rate, base value) in TIMESAT software for both indices time-series, in order to investigate the seasonal behavior of the different vegetation types. Further, we performed wavelet analyses for EVI and NDVI and rainfall time-series in order to detect whether there are anomalies in the series and whether there are coherence and causal relationships between vegetation spectral response and rainfall. PCA showed a clear spectral-temporal separation among forest and savanna physiognomies. Our findings indicated that phenological metrics are efficient in characterizing the seasonal behavior of the Cerrado typologies, and forest-like ones have greater total productivity of green biomass compared to the savanna types. Moreover, we observed coherence between vegetation response and rainfall, in the short-run (32 to 64 and 64 to 128 days). The middle-run wavelet analyses showed a cyclical correlation and coherence between phenology of the physiognomies and rainfall in every 8.5 months. The wavelet NDVI data present an in-phase situation where vegetation leads to rainfall. Conversely, in the long-run, another in-phase is observed and rainfall leads vegetation response. For EVI data, we did not observe any leading phase in the long-run. We concluded that it is possible to separate the Cerrado typologies by their spectral-temporal biophysical responses, enabling the distinction between savanna and forest physiognomies, which show the highest seasonal productivity. It is also possible to conclude

that there is a strong seasonal relationship between rainfall and vegetation biophysical response throughout the time, and that extreme events and long-term trends of rainfall also show coherence with vegetation. These findings suggest that, any rainfall regime change impacts the green biomass productivity of various Cerrado biome physiognomies, from the less productive savannas to the most productive forest patches.

**Keywords:** Remote sensing. Phenology. Cerrado. TIMESAT. NDVI and EVI.

## RESUMO

OLIVEIRA, Brenner de Almeida, M.Sc., Universidade Federal de Viçosa, fevereiro de 2020. **Time-series investigation for correlations between rainfall and phenology in Cerrado (Brazilian savanna)**. Orientadora: Cibele Hummel do Amaral.

A savana brasileira (Cerrado) é o segundo maior bioma do Brasil, depois da Amazônia. A influência do clima neste bioma é acentuada, invernos secos e verões chuvosos determinam as características das tipologias do Cerrado. O efeito do clima na vegetação pode ser avaliado através da variação nas respostas biofísicas de cada tipologia do Cerrado, fornecida por séries temporais de índices espectrais como Índice de Vegetação por Diferenças Normalizadas (NDVI) e Índice de Vegetação Aprimorado (EVI). Este estudo tem como objetivo testar a correlação entre as respostas espectrais das tipologias do Cerrado de 2001 a 2018 e eventos de precipitação no Brasil central. Como objetivos específicos, pretendeu-se separar espectralmente essas fisionomias e caracterizá-las de acordo com suas métricas fenológicas. Assim, foi realizada uma Análise de Componentes Principais (PCA) para as séries temporais MOD13Q1 NDVI e EVI, para testar a separação espectral das tipologias do Cerrado. Extraíu-se as métricas fenológicas (por exemplo, taxa de crescimento, valor base) no software TIMESAT para os dois índices de séries temporais, a fim de investigar o comportamento sazonal dos diferentes tipos de vegetação. Além disso, realizou-se análises de wavelets para EVI e NDVI e séries temporais de chuvas, a fim de detectar se há anomalias na série e se há coerência e relação causal entre a resposta espectral da vegetação e a precipitação. O PCA mostrou uma clara separação espectro-temporal entre as fisionomias das florestas e das savanas. Os resultados indicaram que as métricas fenológicas são eficientes na caracterização do comportamento sazonal das tipologias do Cerrado, e as do tipo floresta têm maior produtividade total da biomassa verde em comparação às do tipo savana. Além disso, observou-se coerência entre a resposta da vegetação e as chuvas, no curto prazo (32 a 64 e 64 a 128 dias). As análises de ondas médias mostraram correlação cíclica e coerência entre a fenologia das fisionomias e chuvas a cada 8,5 meses. As wavelet para dados de NDVI apresentam uma situação em fase em que a vegetação leva à precipitação. De maneira inversa, no longo prazo outra fase é observada onde a precipitação leva à resposta da vegetação. Para os dados do EVI, não foi observado nenhuma fase no longo prazo. Concluiu-se que é possível separar as tipologias de Cerrado por suas respostas biofísicas espectral-temporais, possibilitando a distinção entre savana e fisionomias florestais, as quais

apresentam maior produtividade sazonal. Também é possível concluir que existe uma forte relação sazonal entre a chuva e a resposta biofísica da vegetação ao longo do tempo, e que eventos extremos e tendências de chuva a longo prazo também mostram coerência com a vegetação. Esses achados sugerem que qualquer mudança no regime de chuvas impacta a produtividade da biomassa verde de várias fisionomias do bioma Cerrado, desde as savanas menos produtivas até os fragmentos florestais mais produtivos.

**Palavras-chave:** Sensoriamento remoto. Fenologia. Cerrado. TIMESAT. NDVI e EVI.



## LIST OF FIGURES

<b>Figure 1.</b> Study area location and vegetation domain coverage of Brazilian savanna biome (1: 250,000, base year 2002), according to (SANO <i>et al.</i> , 2007). .....	19
<b>Figure 2.</b> TIMESAT extract metrics: (a) beginning of season, (b) end of season, (c) left 90% level, (d) right 90% level, (e) peak, (f) amplitude, (g) length of season, (h) integral over growing season giving area between fitted function and average of left and right minimum values, (i) integral over growing season giving area between fitted function and zero level (total productivity) (JÖNSSON; EKLUNDH, 2004).....	22
<b>Figure 3.</b> Principal Component Analysis (PCA) of NDVI (A) and EVI (B) in Cerrado typologies. black dots = Seasonal Semi-deciduous Forest dark green = <i>Cerradão</i> ; light blue = Dense Cerrado; red = Typical Cerrado.....	25
<b>Figure 4.</b> Phenological metrics derived from derived from NDVI and EVI data for Typical Cerrado (Typ.cer), Dense Cerrado (Dense.cer), <i>Cerradão</i> (Cer.) and Seasonal Semideciduous Forest (SSF) related NDVI Beginning of season (A), and EVI Beginning of season (B). .....	27
<b>Figure 5.</b> Phenological metrics derived from NDVI data for Typical Cerrado (Typ.cer), Dense Cerarado (Dense.cer), <i>Cerradão</i> (Cer.) and Seasonal Semi-deciduous Forest (SSF) related to NDVI End of season (A), and EVI End of season (B). .....	27
<b>Figure 6.</b> Phenological metrics derived from NDVI data for Typical Cerrado (Typ.cer), Dense Cerrado (Dense.cer), <i>Cerradão</i> (Cer.) and Seasonal Semi-deciduous Forest (SSF) related to NDVI Base value (A), and EVI Base value (B). .....	28
<b>Figure 7.</b> Phenological metrics derived from NDVI data for Typical Cerrado (Typ.cer), Dense Cerrado (Dense.cer), <i>Cerradão</i> (Cer.) and Seasonal Semi-deciduous Forest (SSF) related to NDVI Maximum value (A), and EVI Maximum value (B). .....	28

<b>Figure 8.</b> Phenological metrics derived from NDVI data for Typical Cerrado (Typ.cer), Dense Cerrado (Dense.cer), <i>Cerradão</i> (Cer.) and Seasonal Semi-deciduous Forest (SSF) related to NDVI Length of season (A), and EVI Length of season (B). .....	29
<b>Figure 9.</b> Phenological metrics derived from NDVI data for Typical Cerrado (Typ.cer), Dense Cerrado (Dense.cer), <i>Cerradão</i> (Cer.) and Seasonal Semi-deciduous Forest (SSF) related to NDVI Growth rate (A), and EVI Growth rate (B). .....	29
<b>Figure 10.</b> Phenological metrics derived from NDVI data for Typical Cerrado (Typ.cer), Dense Cerrado (Dense.cer), <i>Cerradão</i> (Cer.) and Seasonal Semi-deciduous Forest (SSF) related to NDVI Senescence rate (A), and EVI Senescence rate (B). .....	30
<b>Figure 11.</b> Phenological metrics derived from NDVI data for Typical Cerrado (Typ.cer), Dense Cerrado (Dense.cer), <i>Cerradão</i> (Cer.) and Seasonal Semi-deciduous Forest (SSF) related to NDVI Amplitude (A), and EVI Amplitude (B). .....	30
<b>Figure 12.</b> Phenological metrics derived from NDVI data for Typical Cerrado (Typ.cer), Dense Cerrado (Dense.cer), <i>Cerradão</i> (Cer.) and Seasonal Semi-deciduous Forest (SSF) related to NDVI Productivity (A), and EVI Productivity (B). .....	31
<b>Figure 13.</b> The coherence between NDVI of the Typical Cerrado and rainfall. ....	33
<b>Figure 14.</b> The coherence between NDVI of the Dense Cerrado and rainfall wavelets. ....	33
<b>Figure 15.</b> The coherence between NDVI of the <i>Cerradão</i> and rainfall wavelets. ....	34
<b>Figure 16.</b> The coherence between NDVI of the Seasonal Semi-Deciduous forest and rainfall wavelets. ....	34

<b>Figure 17.</b> The coherence between EVI of the Typical Cerrado and rainfall wavelets.....	35
<b>Figure 18.</b> The coherence between EVI of the Dense Cerrado and rainfall wavelets. ....	35
<b>Figure 19.</b> The coherence between EVI of the Cerradão forest and rainfall wavelets. ....	36
<b>Figure 20.</b> The coherence between EVI of the Seasonal Semi-Deciduous forest and rainfall wavelets. ....	36
<b>Figure 21.</b> Total rainfall amount in the very short and short-run, D1 (32-64 days) and D2 (4 64-128 days) respectively.....	37
<b>Figure 22.</b> Rainfall wavelet transformation. ....	42
<b>Figure 23.</b> Typical Cerrado wavelet transformation (23A – NDVI and 23B – EVI).....	42
<b>Figure 24.</b> Dense Cerrado wavelet transformation (24A – NDVI and 24B – EVI).....	43
<b>Figure 25.</b> Cerradão wavelet transformation (25A – NDVI and 25B – EVI).....	43
<b>Figure 26.</b> Seasonal Semideciduous Forest (26A – NDVI and 26B – EVI).....	44
<b>Figure 27.</b> Covariance among vegetation indices (27A – NDVI and 27B – EVI) and rainfall, for Typical Cerrado. ....	45
<b>Figure 28.</b> Covariance among vegetation indices (28A – NDVI and 28B – EVI) and rainfall, for Dense Cerrado.....	45

<b>Figure 29.</b> Covariance among vegetation indices (29A – NDVI and 29B – EVI) and rainfall, for Cerradão.....	46
<b>Figure 30.</b> Covariance among vegetation indices (30A – NDVI and 30B – EVI) and rainfall, for Seasonal Semideciduous Forest.....	46
<b>Figure 31.</b> Correlation among vegetation indices (31A – NDVI and 31B – EVI) and rainfall, for Typical Cerrado. ....	47
<b>Figure 32.</b> Correlation among vegetation indices (32A – NDVI and 32B – EVI) and rainfall, for Dense Cerrado.....	47
<b>Figure 33.</b> Correlation among vegetation indices (33A – NDVI and 33B – EVI) and rainfall, for Cerradão.....	48
<b>Figure 34.</b> Correlation among vegetation indices (34A – NDVI and 34B – EVI) and rainfall, for Seasonal Semideciduous Forest.....	48

## LIST OF TABLES

<b>Table 1.</b> Wavelet decomposition scales: D1 + D2 short-run, D3 + D4 middle-run, D5 + S6 long-run. P cycles in days of the time series. ....	24
<b>Table 2.</b> Parameters of the first two axes of the Principal Component Analysis (PCA) of EVI and NDVI of the gaps Savanna types. ....	26

## CONTENTS

1. INTRODUCTION.....	14
2. MATERIAL AND METHODS .....	19
a. Study area .....	19
b. Data acquisition .....	20
c. Data processing.....	20
2.3.1 MODIS Spectral Index.....	20
2.3.2. Rainfall data.....	20
d. Data analysis .....	21
2.4.1 Multivariate analysis .....	21
2.4.2 NDVI and EVI time series.....	21
2.4.3 Wavelet analyses.....	22
2.4.4 ANOVA and Tukey test .....	24
2.4.5 Analyses of variance and correlations.....	24
3. RESULTS .....	25
3.1. Multivariate analyses results .....	25
3.2. Phenological metrics.....	26
3.3. Correlation and coherence between vegetation phenology and rainfall.....	31
4. DISCUSSION .....	38
5. CONCLUSION.....	41
APPENDIX 1 – Wavelet transformation.....	42
APPENDIX 2 – Covariance among vegetation indices and rainfall. ....	45
6. REFERENCE.....	49

## 1. INTRODUCTION

The Neotropical Brazilian Savanna (Cerrado) is the second largest biome in Brazil, following the Amazon (KLINK; MACHADO, 2005). The Cerrado is composed of different phyto-physiognomies, which are distributed in three different main classes: grassland, savanna and forest (RIBEIRO; WALTER, 2008).

As an example of these different classes of Cerrado landscapes, it is possible to highlight the forested class *Cerradão* which corresponds to a “sclerophic mesophilic forest”, and is characterized for an understory formed by small shrubs and herbs, with few kinds of grass. It is characterized by the preferential presence of forest species. From a physiognomic point of view, it is a forest, but floristically it is more like the Cerrado restricted sense (*sensu stricto*) (RIBEIRO; WALTER, 2008). Among other Cerrado’s vegetation, there is the Dense Cerrado and Typical Cerrado. Dense Cerrado is a subtype of predominantly arboreal vegetation, with coverage of 50% to 70% and an average height of five to eight meters. It represents the densest and highest form of Cerrado in a restricted sense. The shrub and herbaceous strata are thinner, probably due to the shading resulting from the higher density of trees. The Typical Cerrado is a subtype of vegetation predominantly arboreal-shrub, with arboreal coverage of 20% to 50% and an average height of three to six meters (RIBEIRO; WALTER, 2008). Besides the traditional Cerrado vegetation, it is possible to find Atlantic forest formations as seasonal semideciduous forests within the domain of this biome (ENCINAS, 2007; FELFILI, 2005).

The Cerrado is a biome of great plant diversity, but it is also highly threatened by anthropic pressure (ANTIQUERA, 2014; GRECCHI, 2014; RATTER, 1997). Currently, the vegetation remained from the 2 million natural and original coverage of this biome is only by around 350,000 ha (BALDUINO *et al.*, 2006). Such high environmental change driven by human pressure, classify the Cerrado as one of the 25 critical global hotspots of biodiversity for conservation (MYERS *et al.*, 2000).

Factors that lead the distribution of Cerrado flora are soil chemistry and physics, water, groundwater depth, geomorphology and topography (RIBEIRO; WALTER, 2008). For Eiten, (1972), Cerrado occur over different topographic conditions and geological formations and is strongly correlated to the climate.

Climate change is currently an urgent global matter of concern, and its effects are perceived in different ways around the planet (COOGAN, 2019; LOO, 2015). In Cerrado, decreased or scarce rainfall combined with high temperatures can lead to an increase in the

wildfire, which when occurs for natural causes is one of the drivers of the diversity in this biome (BUSTAMANTE, 2012). However, the frequency of wildfire has increased, as a result of anthropic pressure, Cerrado *stricto sensu* has been burned every 2-3 years while open areas such as *campo sujo* and *campo limpo* might be burned annually (COUTINHO, 1990). One of the local consequences of repeated wildfire is the decrease in biodiversity (BUSTAMANTE *et al.*, 2012). Fire strongly promotes fire-tolerant species, which replace the species potentially growing in an undisturbed environment, for example, tree species exhibit adaptive traits such as thick bark, ability to heal fire scars, resprouting capability and seed adaptations, this can woodland areas which tend to be more conserved than others (NASI *et al.*, 2002).

Besides fire contribution, rainfall increase has presented an association with a woodland increase. Zhang, (2019) showed that woodland vegetation areas have shown an increase, mainly associated with rainfall increase regime around the world. Then, understanding how rainfall changes might affect the Cerrado typologies is very important regarding phenological studies (CAMARGO, 2011; DE MATTOS, 2002)

Among climate components, water is essential to any ecosystem survival; in plants, it is not different, since it participates in important physiological processes as the transport of nutrients and the photosynthesis (TAIZ; ZEIGER, 2002). Thus, water supply is intrinsically related to biomass production by plants (MUELLER, 2005; TAIZ; ZEIGER, 2002). In another hand, vegetation can contribute to precipitation cycle in a region through evapotranspiration. This phenomenon has been perceived and studied in some regions, like the Amazon forest (ELTHAIR; BRAS, 1994; WRIGHT, 2017). In Cerrado, regarding rainfall, the biome presents a demarcated seasonality with two seasons: the rainy season, from September to April; and the dry season, from April to October, characterized by strong rainfall reduction (ALBUQUERQUE; SILVA, 2008).

The remarkable seasonality of Cerrado, makes it possible to study its phenology – Phenology is the study of the timing of recurring biological events, the causes of their timing concerning biotic and abiotic forces, and interrelation between phases of the same or different species (LIETH, 1974).

The usage of remote sensors to study the phenological behavior of vegetation are efficient (PIAO, 2006; ROSSI, 2019; ZHANG; 2003, 2005). Within the resources provided by remote sensing to study vegetation behavior, spectral vegetation indices (VI's) stand out. Besides allowing powerful spatial and temporal comparisons of vegetation phenology, the VI's are powerful tools for monitoring land-use change (ZHANG, 2003, 2019b).



The most used vegetation index is the Normalized Difference Vegetation Index (NDVI) (ROUSE, 1974), which is efficiently stable for making consistent comparisons of seasonal, inter-annual and long-term variations in vegetation structure, phenology, and biophysical parameters (fraction of absorbed photosynthetically active radiation (f PAR), and biomass) (BOELMAN, 2005; WYLIE, 2002; XU; NIU; TANG, 2018). The strength of the NDVI is in its rationing concept, which reduces many forms of multiplicative noise (illumination differences, cloud shadows, atmospheric attenuation, certain topographic variations) present in multiple bands (HUETE, 2002). However, despite its wide use for several analyses of vegetation, NDVI has some disadvantages (DIDAN; MUNOZ; HUETE, 2015). Among these disadvantages, the pronounced ones are signal saturation over high biomass canopies, and high sensitivity to variations in substrate composition and soil color tone (light or dark) in areas of more sparse or open vegetation (ROSSI *et al.*, 2019).

To overcome the errors generated by NDVI, another vegetation index was created, the Enhanced Vegetation Index (EVI) (HUETE *et al.*, 2002). This index presents better optimization of the vegetation signal and greater sensitivity in high biomass regions, besides an improved vegetation monitoring through a de-coupling of the canopy background signal and a reduction in atmosphere influences (HUETE, 2002; JIANG, 2008). Therefore, is reasonable to conclude that both two indices complement one another in global vegetation studies and boost the identification of changes in vegetation and the collection of biophysical parameters of the canopy (HUETE *et al.*, 2002).

Studies in different environments have already shown through time-series analyses that VI's demonstrate a strong variation of response in the series depending on dry or rainy periods, revealing a strong correlation of the green-up and growth process with rainfall events (DING, 2007; GESSNER, 2013; SCHULTZ, 1993). This way, no matter what type of vegetation, whether natural or cultivated, variables such as rainfall and temperature affect its growth processes (DING, 2007). Thus, observing rainfall behavior over time can be an important resource in understanding the phenological behavior of different vegetation types.

A very handy tool to analyze phenological behavior of vegetation through time series observation is the TIMESAT software Jönsson; Eklundh, (2004), since it permits to extract phenological metrics, as the beginning of the season, end of the season, amplitude and length of the season. Another way to study time series behavior is by using methods such as serial correlation analysis and Fourier transformation (MENENTI, 1993; ROERINK, 2000). The Fourier transform decomposes a signal into orthogonal trigonometric basis functions; thus, it gives the global frequency distribution of the time signal (SANG, 2013; STEINBUCH, 2013).

However, the Fourier transform only retrieves the global frequency content of a signal. Then, the Fourier transform is only useful for stationary and pseudo-stationary signals. The Fourier transform does not give satisfactory results for signals that are highly non-stationary, noisy, or a-periodic (STEINBUCH, 2013). These methods then do not typically satisfy practical needs when applied to series showing non-stationary characteristics, such as hydrological and VI's like NDVI. VI's are time series that act on multi-temporal scales and are typically characterized by patterns like seasonality, trends, and localized abrupt changes (DE BEURS, 2005; NEUPAUER, 2006). The Fourier method still has a major disadvantage on time series, which is the inability to detect anomalies (KIM, 2004).

An alternative to overcome Fourier transformations issues in data analyses is to use wavelet transformations (WT) (CHOUAKRI, 2016; GRAMATIKOV, 1995; SANG, 2013) . The WT's main property is the location of events on the timescale (LABAT, 2000). They are capable of revealing spectral signals details that other techniques fail, such as trends, breakpoints, and discontinuities (STEINBUCH, 2013). As a technique that looks at different sections of the time series with a scale-adjusted window, the WT allows the use of a narrow window to capture the presence of short-lived events (high-frequency variability), such as abrupt changes, while resolving processes that display low-frequency variability in time scale. Such a procedure is known as Multi-Resolution Analysis (MRA), i.e. the signal is studied at a coarse resolution to obtain an overall view of the signal and at in increasing resolutions to see increasingly finer details (BURKE-HUBBARD, 1998).

The potential use of MRA over time series has been studied and good results have been shown regarding to the ability for identifying changes in the temperature of the surface air and the areas affected by this variation, and to separate different types of vegetation (PERCIVAL, 2004). Another potential use of MRA is WT-based MRA, which makes it possible to analyze the dynamics of vegetation based on different temporal scales, a study performed by Martínez; Gilabert, (2009) for example, used wavelet analyses on NDVI time series to capture and explain changes in broadleaf forest, coniferous forest, rice, Mediterranean semiarid scrubland, and alpha-steppes vegetation phenology intra-and inter-annual.

The increase of woodland areas on the savannas domain has been noted, mainly associated with rainfall increase in those areas (ZHANG *et al.*, 2019a), also it is also known that in some regions like the Amazon, vegetation physiologic process are is strongly related to rainfall events (SPRACKLEN, 2012; WRIGHT, 2017). Then, questions to be answered are: is it possible to distinguish the Cerrado typologies by their phenological behavior? Is there a correlation between rainfall and Cerrado green biomass production? To answer these questions,

we analyzed 2001-2018 time-series of NDVI and EVI from MODIS images to separate the Cerrado typologies by their spectral-temporal response and characterize their differences through phenological metrics. Then, we tested the correlation and coherence between rainfall and spectral response of the Cerrado types.

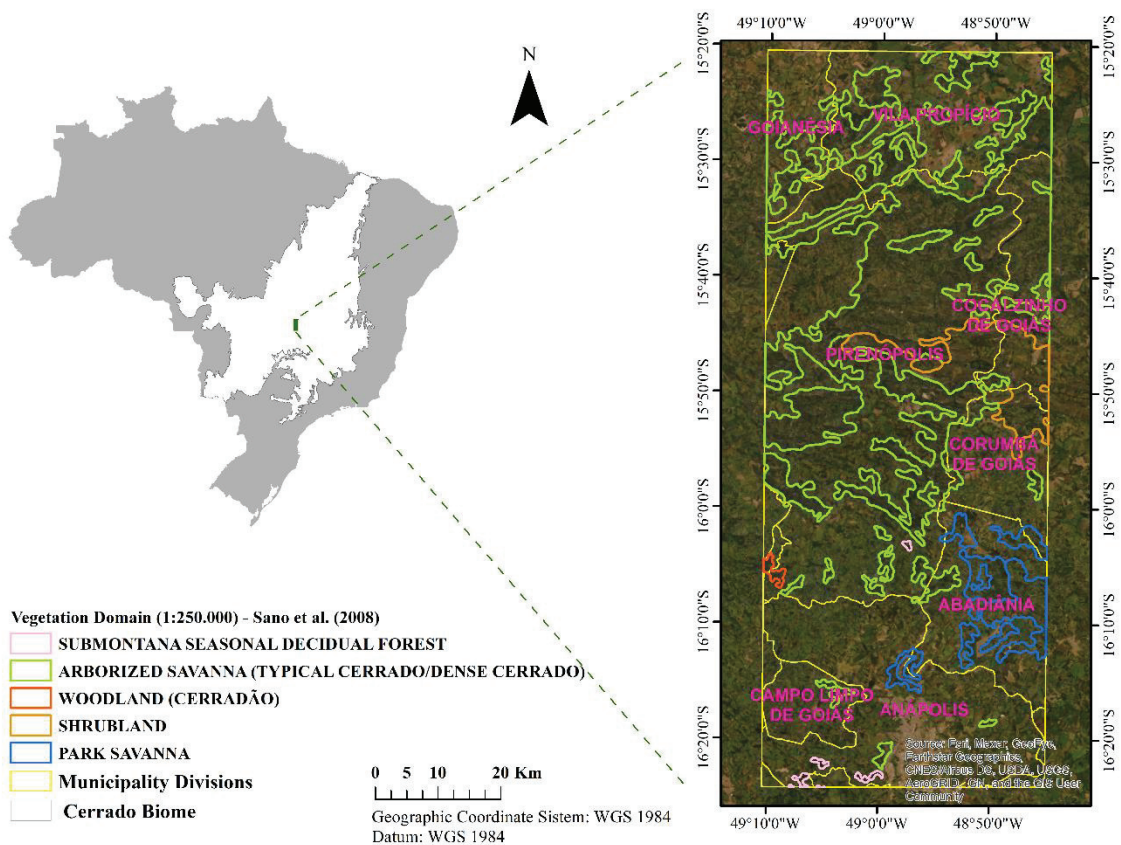
## 2. MATERIAL AND METHODS

### a. Study area

The study area (Figure 1) is located between the coordinates  $15^{\circ}23'36''$  and  $16^{\circ}18'57''$  S and  $48^{\circ}46'53''$  and  $49^{\circ}7'13''$  W, and has 363,000 hectares. It comprises part of the municipalities of *Goianésia*, *Vila Propício*, *Pirenópolis*, *Cocalzinho de Goiás*, *Corumbá de Goiás*, *Abadiânia*, *Anápolis* and *Campo Limpo de Goiás*, in the state of *Goiás*, Brazilian Midwest. The Cerrado Ecomuseu (Brazilian savanna Ecological Museum), which has 806 ha is within the boundaries of the proposed area and covers part of the municipalities of *Pirenópolis*, *Cocalzinho de Goiás*, *Corumbá de Goiás* and *Abadiânia*.

The region's climate is tropical with a dry season megathermal (Aw) or humid tropical (A), with the savanna climate subtype, with dry winter and peak summer precipitation (w) according to Köppen-Geiger climate classification (DA SILVA *et al.*, 2008).

Figure 1. Study area location and vegetation domain coverage of Brazilian savanna biome (1:250,000, base year 2002), according to (SANO *et al.*, 2007).



Source: Author's own

## **b. Data acquisition**

We used 16-day composited images of Normalized Difference Vegetation Index - NDVI, Enhanced Vegetation Index - EVI (NDVI-EVI/MOD13Q1 product at 250 m spatial resolution) and pixel reliability (437 images each), tile h13v10, from 2001 to 2018, from the Moderate Resolution Imaging Spectroradiometer (MODIS) for the vegetation spectral response analyses. These composite images contain the best possible observations, on a per-pixel basis, acquired along a 16-day period, based on parameters such as cloud and aerosol contamination and viewing geometry (DIDAN; MUNOZ; HUETE, 2015). The data is available in sinusoidal projection and HDF file format and was acquired with the aid of the MODISTsp R package (BUSETTO; RANGHETTI, 2016). For rainfall analysis, we used daily data for the period of 2001 to 2018, from the conventional station located in Pirenópolis - GO (OMM: 83376). These data are available at the National Institute of Meteorology (INMET) website (<http://www.inmet.gov.br/portal/index.php?r=bdmep/bdmep>).

## **c. Data processing**

### **2.3.1 MODIS Spectral Index**

With the MODIS products, we extracted the NDVI and EVI data separately from the HDF file and converted them to an appropriate geographic projection through the MODIS reprojection tool (JUSTICE *et al.*, 2002). Then, we selected the pure pixels, i.e. totally within the boundaries, of Cerrado physiognomies polygons by using ArcGIS 10.6 (ESRI, 2013). We identified the vegetation physiognomies in the field and delimited them with the aid of higher resolution images, as presented in (QUINTÃO, 2018). We used only polygons with areas larger than 6.25 ha, which corresponds to the area of one pixel 250 x 250 m of MODIS images. Thus, we selected the physiognomies that had fragments with the minimum of 10 pure pixels as follow: Typical Cerrado (TC) 43 pixels, Dense Cerrado (DC) 58 pixels, *Cerradão* (CE) 33 pixels, and Seasonal Semi-deciduous Forest (SSF) 178 pixels. Then, we extracted NDVI and EVI spectral response values for the different Cerrado physiognomies using the package labgeo (FILHO, 2018) in R 3.5.3. The function `extract_data_point` extracts desired information from overlapping images for a defined location (points), which provide NDVI and EVI time series of the location of interest.

### **2.3.2. Rainfall data**

We divided precipitation data into 16-day groups and sum the values of collected data in each group for each of these periods, then we summed the periods of each year, the result was an annually accumulated precipitation temporal series. Thus, we performed a temporal

change on rainfall data from daily values to each 16-day total value composite, such action was necessary to compare rainfall data with NDVI and EVI spectral responses. These procedures were made using the R `seq` and `sum` functions (R CORE TEAM, 2018).

#### **d. Data analysis**

##### **2.4.1 Multivariate analysis**

Since the specificities of distinct vegetation types commonly encompass spectral particularities (ASNER, 2011; RAPINEL, 2019), we compared the indices EVI and NDVI among the Cerrado typologies. We achieved this by carrying out a principal component analysis (PCA) for the whole time series of EVI and NDVI using the `rda` function with 999 permutations Bellier et al., (2012) in the package `vegan` Oksanen *et al.*, (2019), R version (3.5.3) (R CORE TEAM, 2018). The time series were already smoothed through the Savitzky–Golay function (see section 2.4.2 Time Series NDVI and EVI). Further, we calculated the F statistic for (a) RDA model by using the `anova` function in R in order to test for significant variation of the indices among Cerrado physiognomies. The overall percentage of explanation of the RDA for each index was demonstrated by the adjusted R-squared using the function `RsquareAdj` of the package `vegan` (OKSANEN *et al.*, 2019).

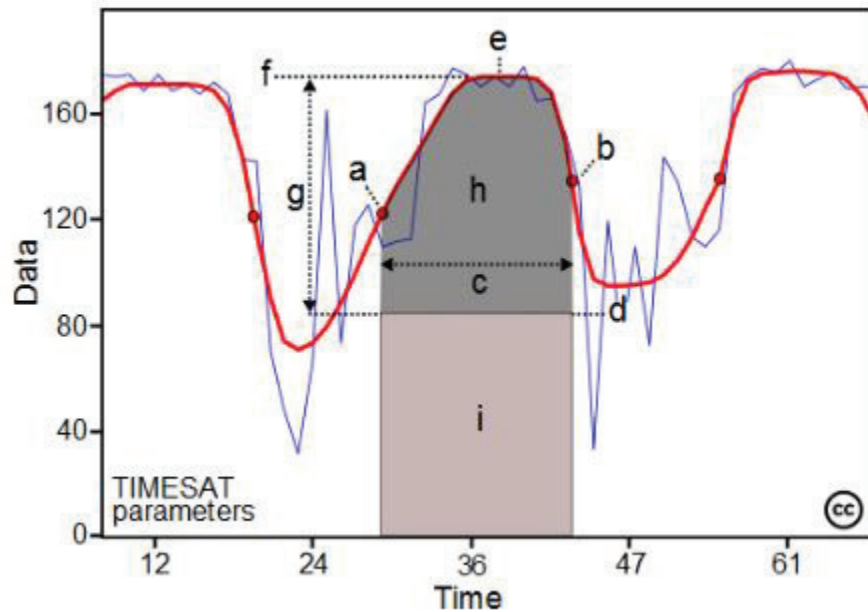
##### **2.4.2 NDVI and EVI time series**

We used TIMESAT 3.3 functions (Jönsson; Eklundh, 2004), to make mathematical adjustments to NDVI and EVI time series and extract phenological metrics. TIMESAT's procedure consists of modeling functions locally at each set of points in the vegetation index time series, providing a better representation of the maximum and minimum (ALMEIDA *et al.*, 2015). The MOD13 pixel reliability band was used to weight each pixel in the data series, where the zero value of this band (good quality data) had total weight (1.0), the values 1 and 2 (ice/snow) were half weight (0.5), and value 3 (clouds) received a 0 weight. Even or sites do not have snow/ice locations it still needed to set up these values for the proper tool functioning.

The function adjustment parameters used for data smoothing/filtering were: Savitzky-Golay filter with 4-point window size in 2 adjustment steps, 2-point adaptive strength; STL-replace spike method, for seasonal parameter and start and end of season that we used the default 0.5. The method used to determine the start and end of the season was the seasonal amplitude, which is defined between the base level and the maximum value for each individual season. The start occurs when the left part of the fitted curve has reached a specified fraction of the amplitude, counted from the base level. Likewise, the end of the season is described for the right side of the curve.

The metrics extracted from TIMESAT include the beginning and end of the growing season, seasonal length, NDVI amplitude, large integrated value (total vegetation production), maximum NDVI and EVI recorded values, and the amplitude (Intra-annual variability (i.e. seasonality) of primary production) (Figure 2). The phenological metrics addressed in this study are presented in Table 1.

Figure 2. TIMESAT extract metrics: (a) beginning of season, (b) end of season, (c) left 90% level, (d) right 90% level, (e) peak, (f) amplitude, (g) length of season, (h) integral over growing season giving area between fitted function and average of left and right minimum values, (i) integral over growing season giving area between fitted function and zero level (total productivity).



Source: (Jönsson; Eklundh, 2004)

### 2.4.3 Wavelet analyses

Wavelet transform is a mathematical method that allows us to analyze non-stationary signals in time and frequency by decomposing time series as well as indicating the frequencies in the signal and the time interval. Further, the technique consists of dilating or compressing a mother function in a set of small waves capable of detecting data series high and low frequencies, allowing analysis at various time scales (GRAPS, 1995).

The wavelet function is mathematically defined on a scale  $a$  and position  $b$ , where  $a$  and  $b$  are real values, and  $a > 0$  as:

$$\psi_{(a,b)}(t) = \frac{1}{\sqrt{a}} \psi\left(\frac{t-b}{a}, a > 0, b \in R. \quad (1)$$

We used the Morlet wavelets to perform the analyses. For Morlet the mother wavelet is given by:

$$\phi(t) = \left( e^{-tft} - e^{-\frac{1}{2}f^2} \right) e^{-\frac{1}{2}t^2} \quad (2)$$

The general Morlet wavelet is created from the mother Morlet wavelet by scaling by  $s$  and displacing by  $l$ :

$$\phi_{sl}(t) = |s|^{-\frac{1}{2}} \left( e^{-tf\left(\frac{t-l}{s}\right)} - e^{-\frac{1}{2}f^2} \right) e^{-\frac{1}{2}\left(\frac{t-l}{s}\right)^2} \quad (3)$$

Both scale  $s$  and displacement  $l$  run from  $-\infty$  to  $\infty$ .

The ability to capture features across a wide range of frequencies and events that are local in time makes the wavelet transform an robust tool to deal with the time-varying characteristics found in most real-world time series (GALLEGATI *et al.*, 2011). Moreover, this approach considers the non-stationary problems as an intrinsic property of data and does not require to be solved by data processing. Therefore, we tested the non-stationarity condition of data, by using the Autocorrelation function test (ACF) and the Kwiatkowski-Philips-Schmidt-Shin (KPSS) using R version (3.5.3). We did the MRA (multi-resolution analysis) for NDVI, EVI and rainfall time series by using the `mra` function with MODWT (Maximum Overlap Discrete Wavelet Transform) as method `waveslim` package (WHITCHER, 2013) R version (3.5.3)

In these experiment we performed a MRA (Multi-Resolution Analysis) of order  $J = 6$  on TC, DC, CE, SSF and precipitation data by using the MODWT based upon the (Mallat, 2009) least asymmetric (LA) wavelet filter. In the figures (APPENDIX 1), the orthogonal components (D1; D2;...; D6) are plotted, which in detail represent the different frequency components of the original series and a smoothed component i.e. S6. The energy explanation (spectral sign distribution) of the Cerrado physiognomies studied and rainfall is in table 1. We also performed wavelet analyses to verify the covariance, correlation and coherence between the rainfall and NDVI and EVI time series.



Table 1. Wavelet decomposition scales: D1 + D2 short-run, D3 + D4 middle-run, D5 + S6 long-run. P cycles in days of the time series.

Level (j)	Wavelet Scales	P (days)
1	D1 (2-4/ 16 days cycles)	32-64
2	D2 (4-8/ 16 days cycles)	64-128
3	D3 (8-16/ 16 days cycles)	128-256
4	D4 (16-32/ 16 days cycles)	256-512
5	D5 (32-64/ 16 days cycles)	512-1,024
6	D6 (64-128/ 16 days cycles)	1024-2048
7	S6 (> 128/ 16 days cycles)	>2048

#### 2.4.4 ANOVA and Tukey test

We tested for the null hypothesis of the non-significant difference of the phenological metrics (beginning, end, and length of season; base and maximum values of EVI and NDVI; L-derivative (growth rate), L-integer (total vegetation production) and amplitude) among the Cerrado physiognomies by computing an ANOVA One Way with the function `aov` R version (3.5.3). Then, we compared the pairwise means among the physiognomies using contrasts of Tukey from the function `TukeyHSD`. All the tests were performed considering  $p < 0.05$  as the significance decision threshold. Further, we showed graphically the outcomes of these tests with Boxplots constructed using the function `geom_boxplot` of the package `ggplot2` (WICKHAM; WINSTON, 2019).

#### 2.4.5 Analyses of variance and correlations

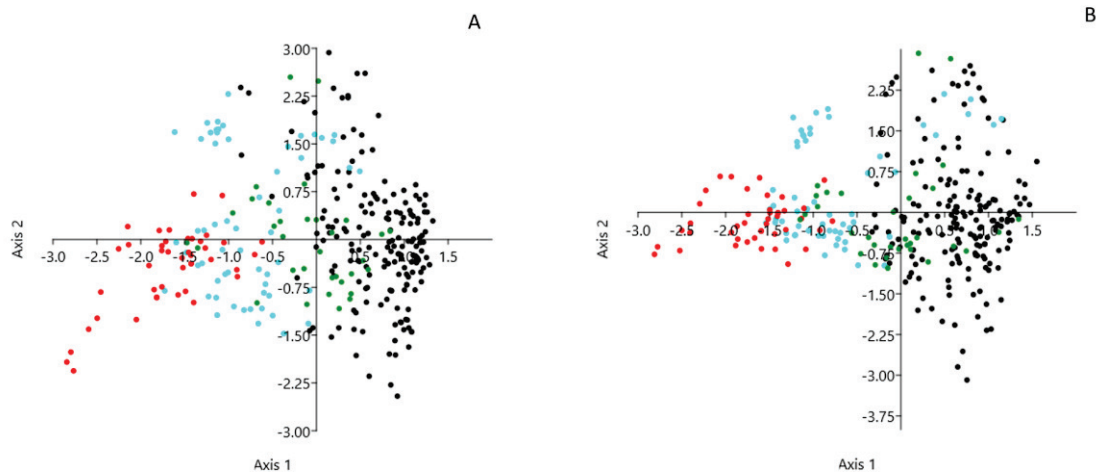
To estimate the multiscale correlation and covariance among the time series of EVI, NDVI and rainfall of the Cerrado physiognomies, we used the functions `wave.correlation` and `wave.covariance` from the package `waveslim`, R version (3.5.3) (R CORE TEAM, 2018; WHITCHER, 2019). Since the time-independent wavelet variance regards to the squared wavelet coefficients across each scale, we previously withdrew the noise of EVI and NDVI by decomposing the variance for a non-stationary process (PERCIVAL DONALD, 1995).

### 3. RESULTS

#### 3.1. Multivariate analyses results

We found a distinct spectral separation by EVI and NDVI among the Cerrado physiognomies in PCA along its two-axis (Figure 3) with significance by the F test (NDVI:  $F = 142.17$ ,  $p = 0.01$ ; EVI:  $F = 119.78$ ,  $p = 0.01$ ). Axis 1 of the PCA holds the higher eigenvalue and explained most of the variation observed in the EVI and NDVI separation among the physiognomies (Table 2). For both EVI and NDVI (Figures 3A and 3B respectively), Axis 1 shows a clear gradient from the Typical Cerrado in the extreme horizontal left side to Seasonal Semi-deciduous Forest in the extreme right side with Dense Cerrado and *Cerradão* among them. On the other hand, Axis 2 holding the second larger eigenvalue and portion of variance explained was mostly correlated with DC and SSF for both EVI and NDVI. CE and SSF were closer in axis 1 for both EVI (Figure 3A) and NDVI (Figure 3B), while DC and TC were more segregated in axis 2.

Figure 3. Principal Component Analysis (PCA) of NDVI (A) and EVI (B) in Cerrado typologies. black dots = Seasonal Semi-deciduous Forest dark green = *Cerradão*; light blue = Dense Cerrado; red = Typical Cerrado.



Source: Author's own

Table 2. Parameters of the first two axes of the Principal Component Analysis (PCA) of EVI and NDVI of the gaps Savanna types.

	Index	PC1	PC2
Eigenvalues	NDVI	0.74	0.24
	EVI	0.53	0.22
Percentage of variance explained	NDVI	42.54	14.24
	EVI	39.82	16.57
Cumulative proportion	NDVI	0.75	0.81
	EVI	0.72	0.79
Adjusted R-squared	NDVI	0.57	
	EVI	0.53	

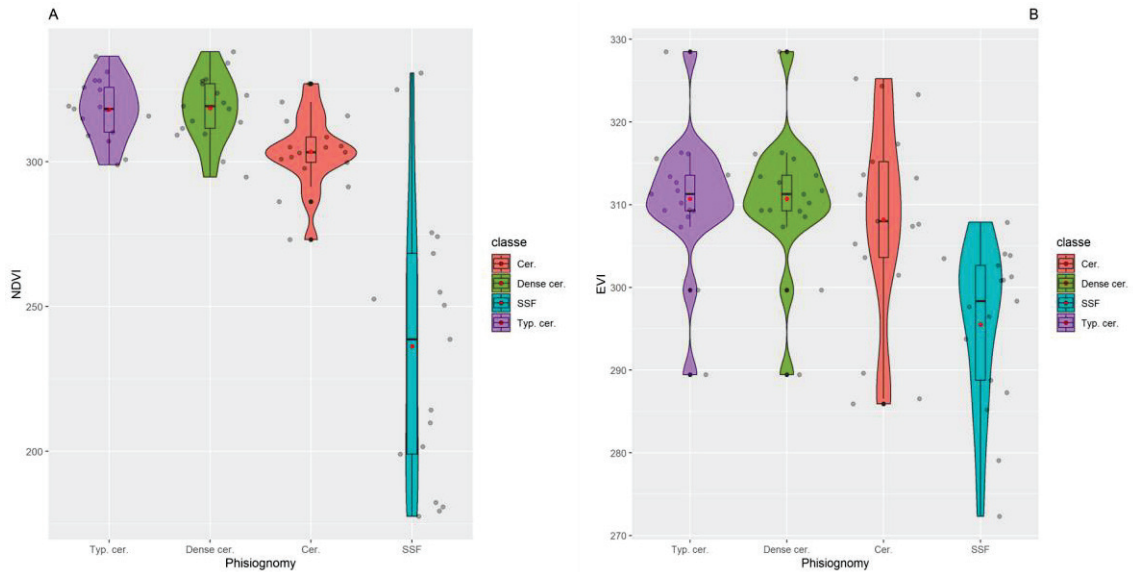
### 3.2. Phenological metrics

We found different patterns of spectral response in the metrics derived from the NDVI and EVI data for all the Cerrado typologies. For NDVI, the beginning of the growing season happens by around the days 300 and 320 (October - November) on average for all the Cerrado's physiognomies, the SSF had a smaller mean around the day 236 (August) (Figure 4A). For EVI, the beginning of the season seems to happen around the days 300 and 310 (October - November) for all the vegetation physiognomies studied (Figure 4B). Regarding End of the season, all the Cerrado vegetations show means around the day 550 (July) for the NDVI while SSF has a smaller mean around the day 476 (April) (Figure 5A). EVI shows values of End of the season also decreasing gradually from savanna vegetation to forested vegetation, thus TC shows a mean by day 547 (July) and SSF 476 (Figure 5B). Base and maximum values (Figures 6 and 7, respectively) show a pattern with the values increasing with vegetation gradient cover. Thus, SSF shows the highest values, while TC got the lowest values. CE and DC appear with intermediate values for maximum values of NDVI (Figure 7A); then, these two vegetation types are better characterized by the EVI index for this metric (Figure 7B).

For the length of season EVI can characterize better the vegetation since it is possible to note that there is a stronger separation between the mean values of savanna and forest physiognomies in this metric (Figure 8B). The growth rate does not show a statistical difference for most Cerrado physiognomies under NDVI and EVI, excepting TC, which presents a lower growth rate under EVI (Figure 9B). For senescence rate EVI (Figure 10B) shows increasing values from savanna to forest-like vegetation. The NDVI amplitude shows higher values for savanna vegetation and was notably separated from CE and SSF physiognomies (Figure 11A). EVI data shows a different pattern where TC has lower values of amplitude (Figure 11B). The productivity metric from NDVI and EVI data (Figures 12A and 12B, respectively) shows the

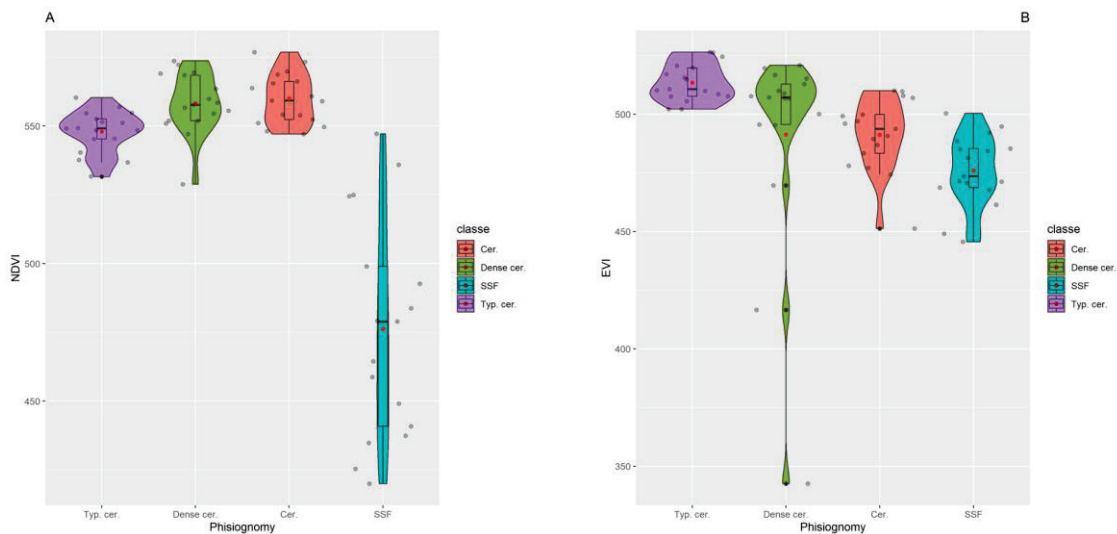
same pattern, i.e., the highest values for SSF and the lowest values for TC. However, productivity under NDVI shows no statistical difference between CE and SSF, the same happen for CE and DC under EVI.

Figure 4. Phenological metrics derived from derived from NDVI and EVI data for Typical Cerrado (Typ.cer), Dense Cerrado (Dense.cer), *Cerradão* (Cer.) and Seasonal Semideciduous Forest (SSF) related NDVI Beginning of season (A), and EVI Beginning of season (B).



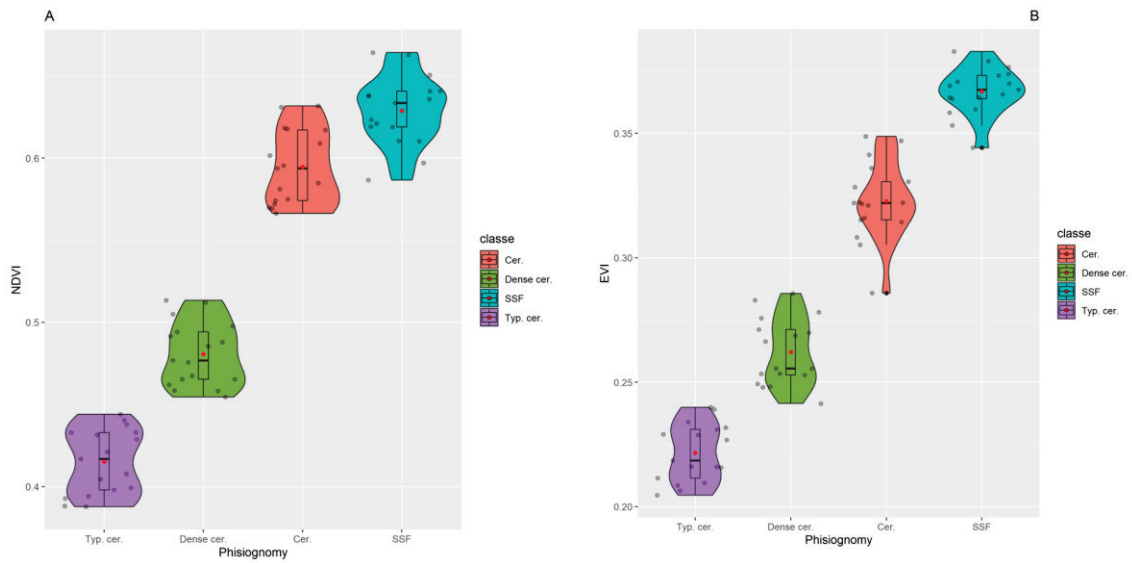
Source: Author's own

Figure 5. Phenological metrics derived from NDVI data for Typical Cerrado (Typ.cer), Dense Cerrado (Dense.cer), *Cerradão* (Cer.) and Seasonal Semi-deciduous Forest (SSF) related to NDVI End of season (A), and EVI End of season (B).



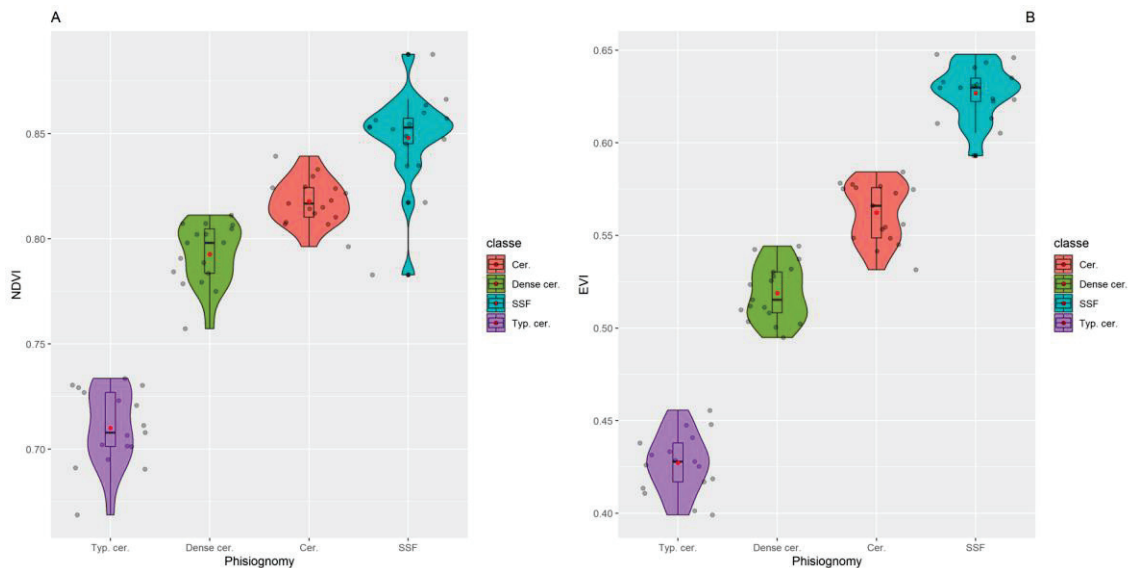
Source: Author's own

Figure 6. Phenological metrics derived from NDVI data for Typical Cerrado (Typ.cer), Dense Cerrado (Dense.cer), *Cerradão* (Cer.) and Seasonal Semi-deciduous Forest (SSF) related to NDVI Base value (A), and EVI Base value (B).



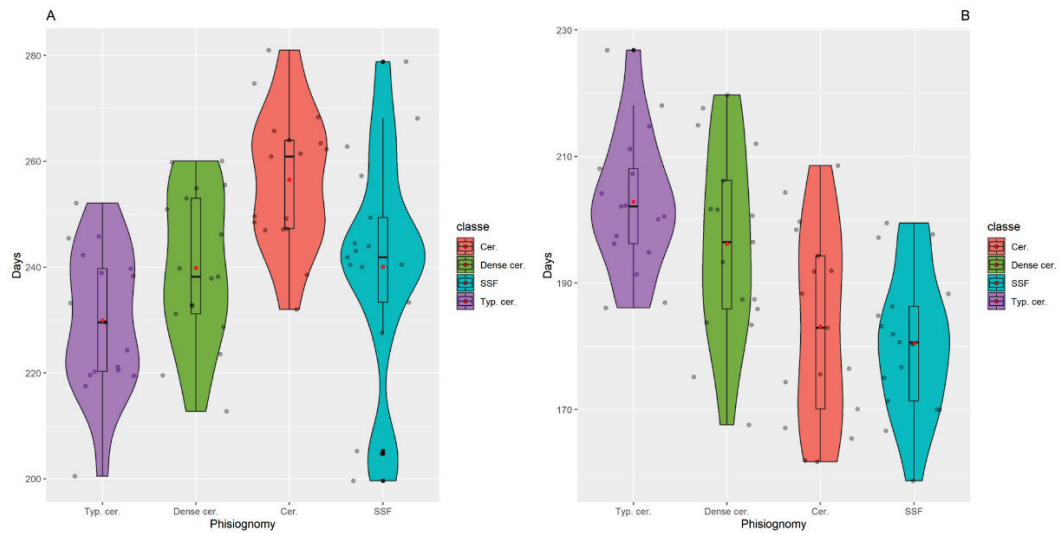
Source: Author's own

Figure 7. Phenological metrics derived from NDVI data for Typical Cerrado (Typ.cer), Dense Cerrado (Dense.cer), *Cerradão* (Cer.) and Seasonal Semi-deciduous Forest (SSF) related to NDVI Maximum value (A), and EVI Maximum value (B).



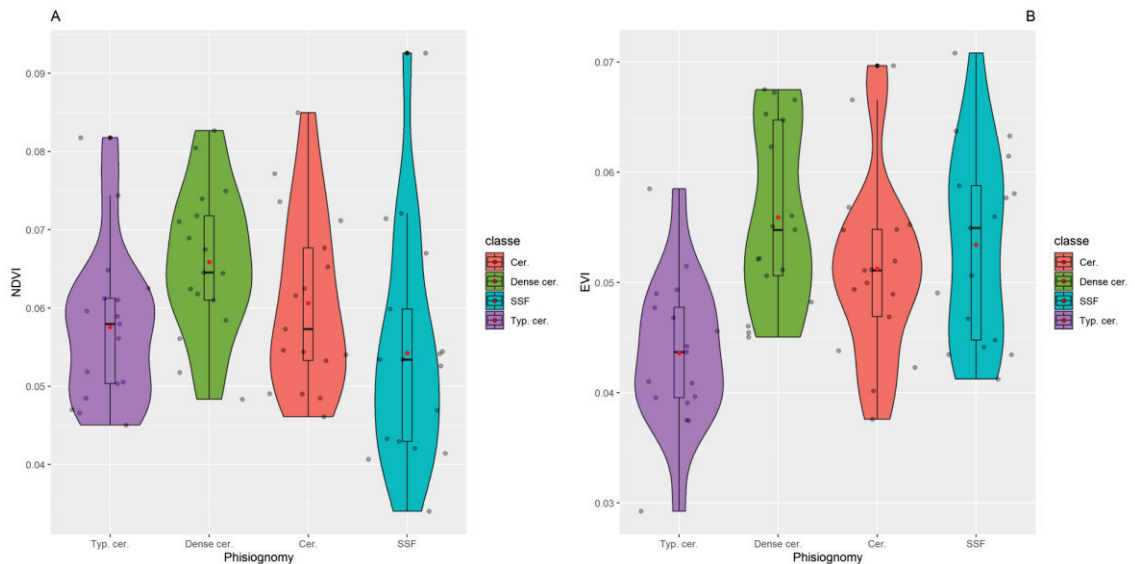
Source: Author's own

Figure 8. Phenological metrics derived from NDVI data for Typical Cerrado (Typ.cer), Dense Cerrado (Dense.cer), *Cerradão* (Cer.) and Seasonal Semi-deciduous Forest (SSF) related to NDVI Length of season (A), and EVI Length of season (B).



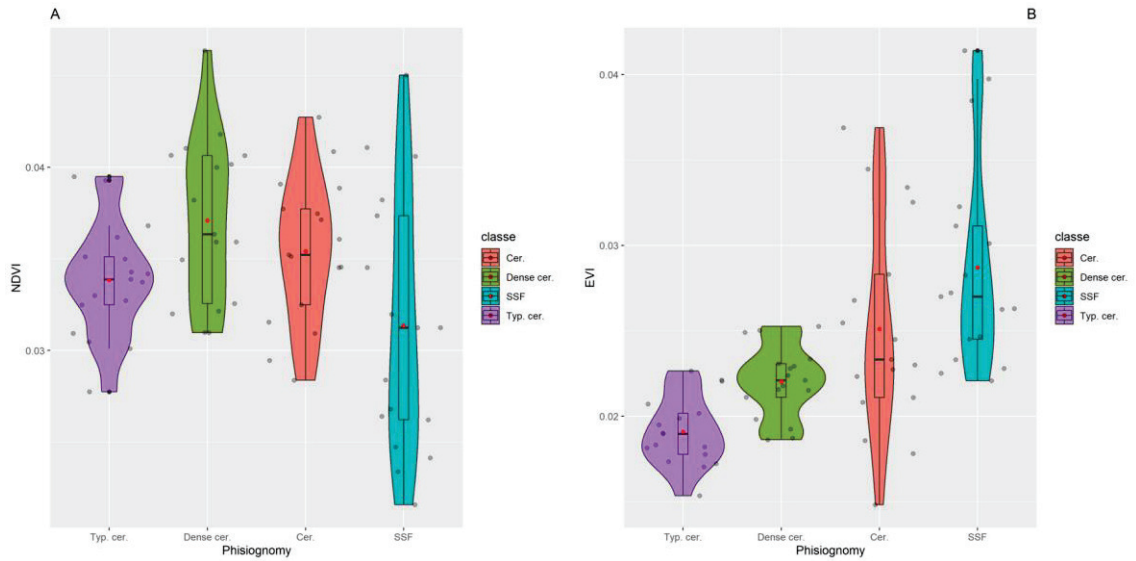
Source: Author's own

Figure 9. Phenological metrics derived from NDVI data for Typical Cerrado (Typ.cer), Dense Cerrado (Dense.cer), *Cerradão* (Cer.) and Seasonal Semi-deciduous Forest (SSF) related to NDVI Growth rate (A), and EVI Growth rate (B).



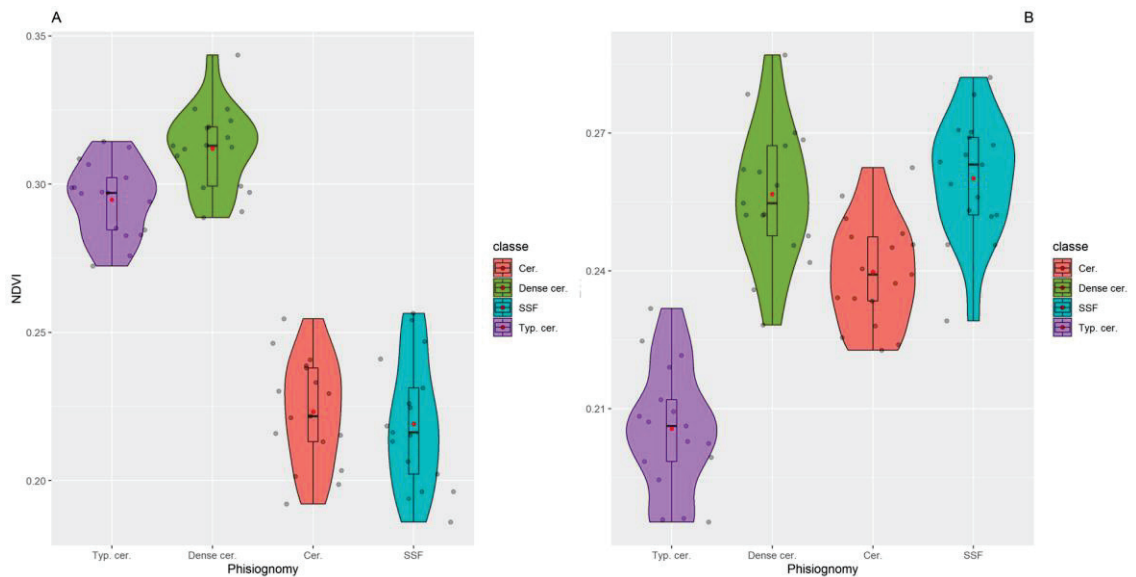
Source: Author's own

Figure 10. Phenological metrics derived from NDVI data for Typical Cerrado (Typ.cer), Dense Cerrado (Dense.cer), *Cerradão* (Cer.) and Seasonal Semi-deciduous Forest (SSF) related to NDVI Senescence rate (A), and EVI Senescence rate (B).



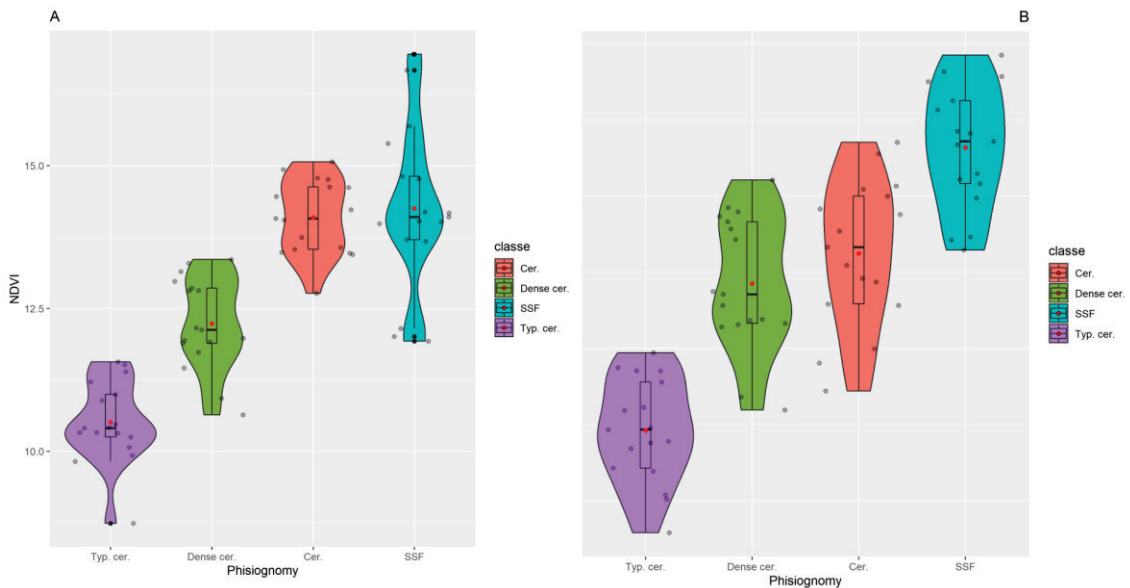
Source: Author's own

Figure 11. Phenological metrics derived from NDVI data for Typical Cerrado (Typ.cer), Dense Cerrado (Dense.cer), *Cerradão* (Cer.) and Seasonal Semi-deciduous Forest (SSF) related to NDVI Amplitude (A), and EVI Amplitude (B).



Source: Author's own

Figure 12. Phenological metrics derived from NDVI data for Typical Cerrado (Typ.cer), Dense Cerrado (Dense.cer), *Cerradão* (Cer.) and Seasonal Semi-deciduous Forest (SSF) related to NDVI Productivity (A), and EVI Productivity (B).



Source: Author's own

### 3.3. Correlation and coherence between vegetation phenology and rainfall

We used the wavelet analysis to examine the covariance (APPENDIX 2) and correlation (APPENDIX 3) that exist among Cerrado physiognomies and rainfall during the period studied. The result shows that in the short, long, and very long-run no covariance exists between rainfall and Cerrado physiognomies, whereas, there is a positive covariance in the medium-run which corresponds in scale to D4 (from 256 to 512 days). We also found the strongest (and positive) correlation among the variables in the medium-run period, with a gradual decrease in the long period being observed. The covariance and correlation results show that the association between Cerrado typologies and rainfall is strong and positive, and with a seasonal pattern mainly.

We used the wavelet coherence to analyze the causal association among the variables. It offers the common power (features) and comparative phase of various time sequences in present time-frequency space (Figures 13-20). In these figures, the cone of influence COI (gray arc) presents information that has statistical significance; the time is displayed on the horizontal axis, while the vertical axis shows the frequency (the lower the frequency, the higher the scale). Regions in time-frequency space where the two time-series co-vary are located by the wavelet coherence. Warmer colors (red) represent regions with significant interrelation, while colder

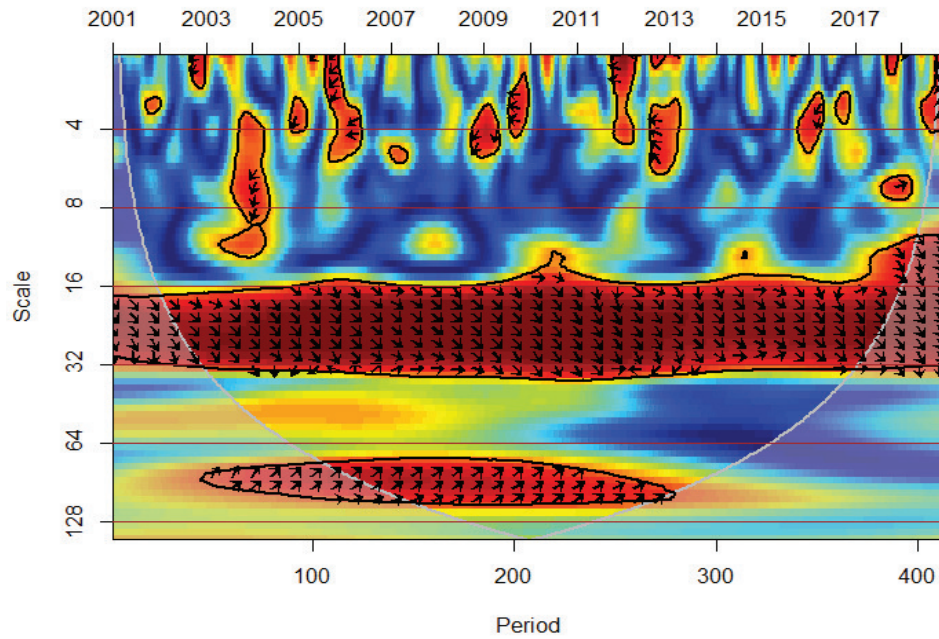


colors (blue) signify lower dependence between the series. Cold regions beyond the significant areas represent time and frequencies with no dependence in the series. An arrow in the wavelet coherence plots represents the lead/lag phase relations between the examined series. A zero-phase difference means that both time-series move together on a particular scale. Arrows point to the left when the time-series are in (anti-phase), arrows point to the right when they are (in-phase). The in-phase state indicates that they move in the same direction, and anti-phase means that they move in the opposite direction. Arrows pointing to the right-down or left-up indicate that the first variable (X) is leading, while arrows pointing to the right-up or left-down show that the second variable (Y) is leading.

The short-run D1 and D2 (Cycles of 32 to 128 days) shows some little zones of coherence for most of the Cerrado physiognomies (Figures 13-20). However, these anomalous, extreme events in the short-run show no pattern of leading phase. We calculated the amount of rainfall over the study area for the period, to see the possible influence of anomalous rainfall events in these short-run coherence zones, the results show a minimum of 479.5 mm a maximum of 1575 mm and a mean of 1119.4 mm; and some years as 2004, 2005, 2007 and 2013 got an amount of rainfall very higher than average when compared to the other years (Figure 21).

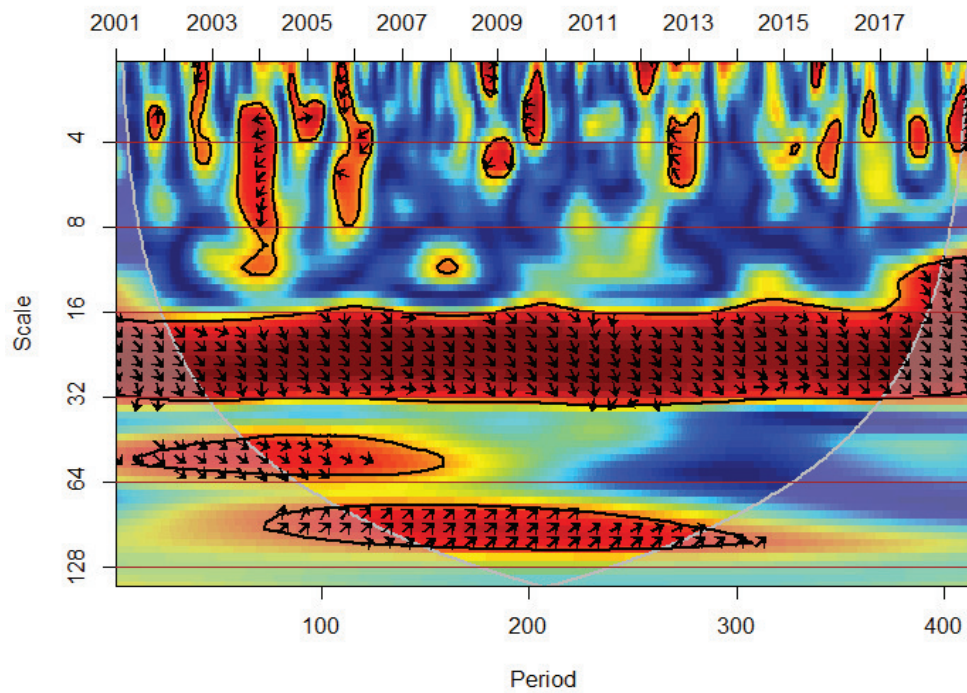
The strongest coherence is seen in the medium-run D4 (from 256 to 512 days) days or every 8.5 months to 1,5 years) for both indices and for all vegetation physiognomies and an in-phase situation is led by vegetation. On the other hand, in the long-term (512 to 1024 days) and very long-term (1024 to 2048 days) an inverse leading phase situation is observed where precipitation leads the coherence generally in the middle of the time series.

Figure 13. The coherence between NDVI of the Typical Cerrado and rainfall.



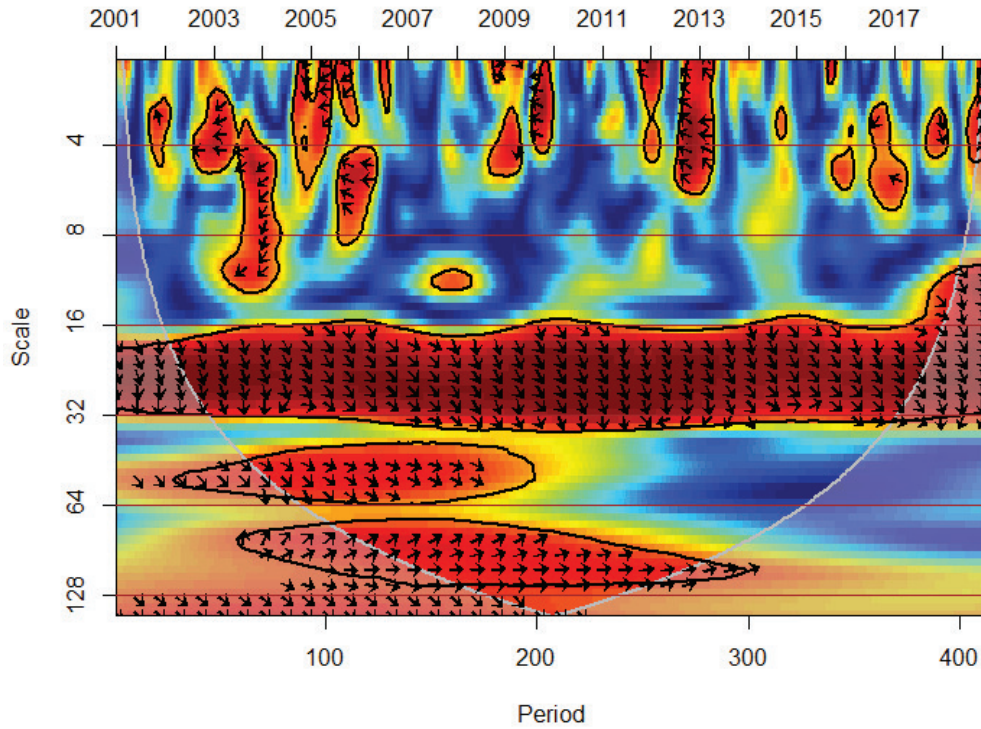
Source: Author's own

Figure 14. The coherence between NDVI of the Dense Cerrado and rainfall wavelets.



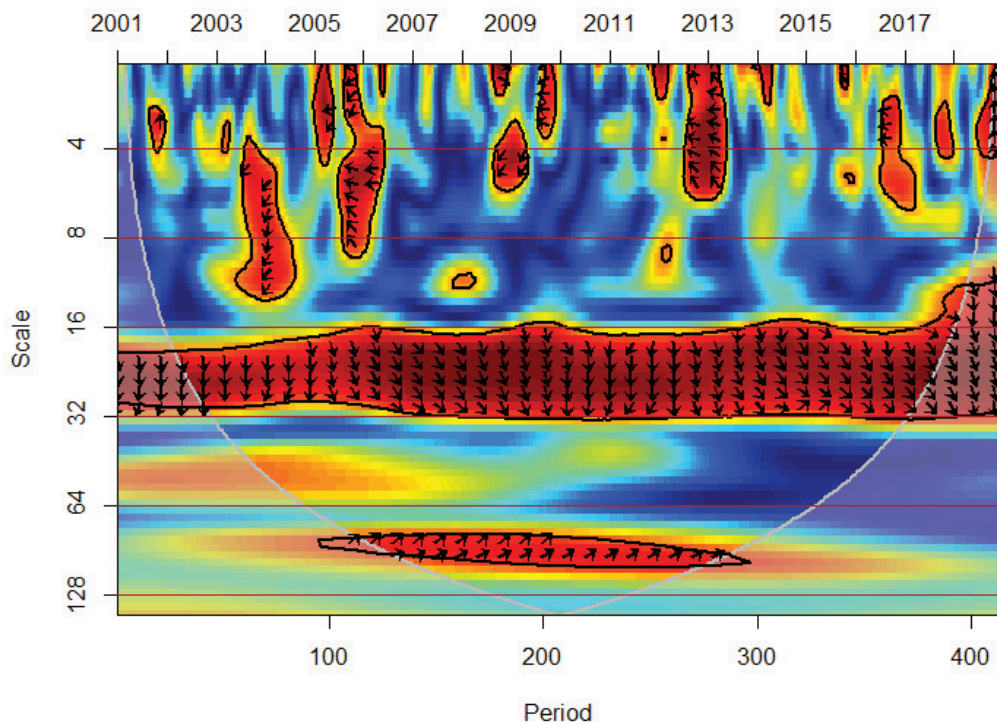
Source: Author's own

Figure 15. The coherence between NDVI of the *Cerradão* and rainfall wavelets.



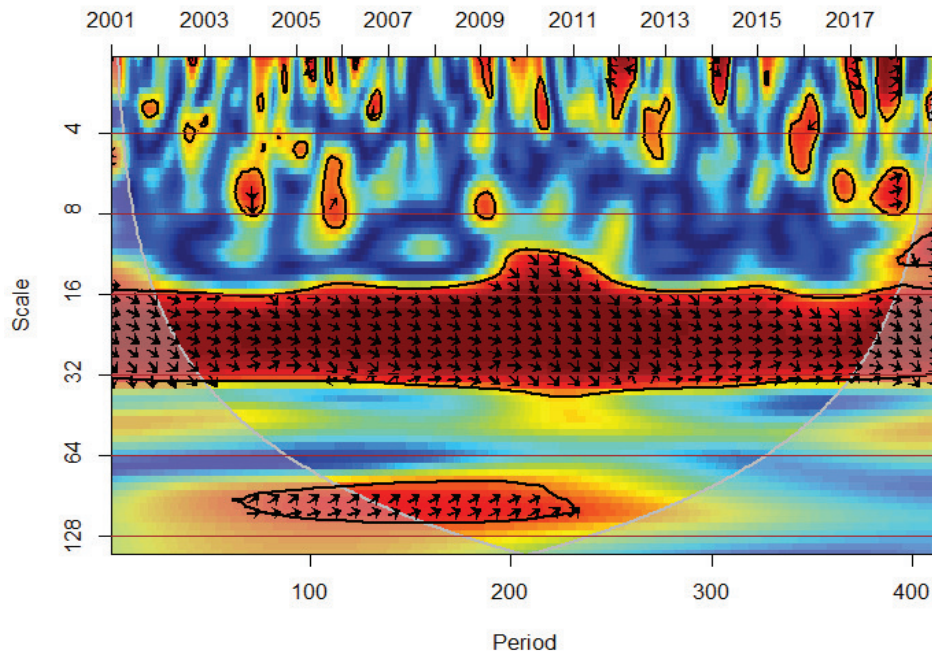
Source: Author's own

Figure 16. The coherence between NDVI of the Seasonal Semi-Deciduous forest and rainfall wavelets.



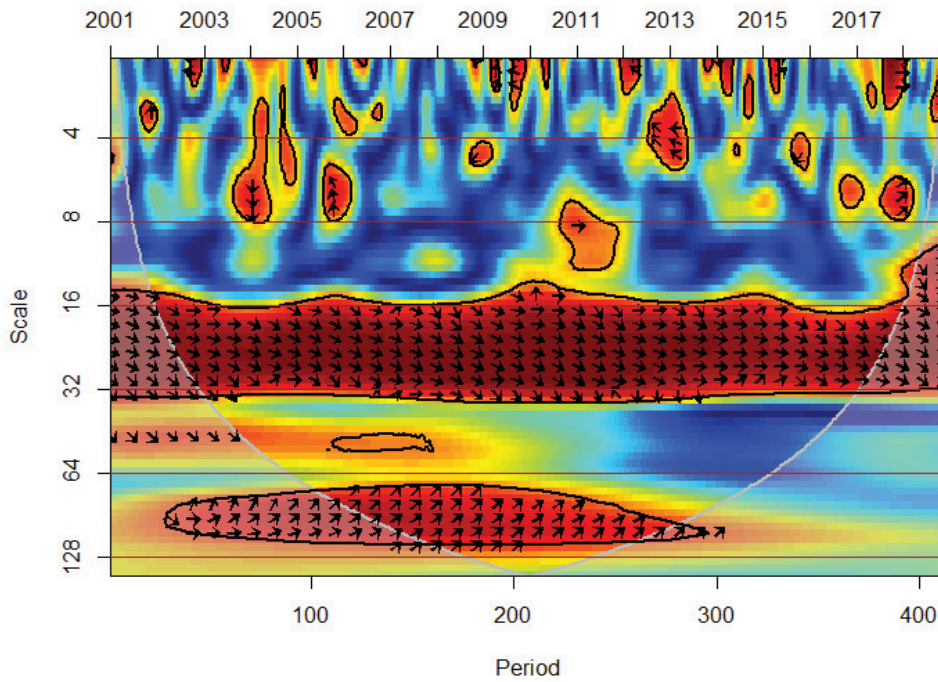
Source: Author's own

Figure 17. The coherence between EVI of the Typical Cerrado and rainfall wavelets.



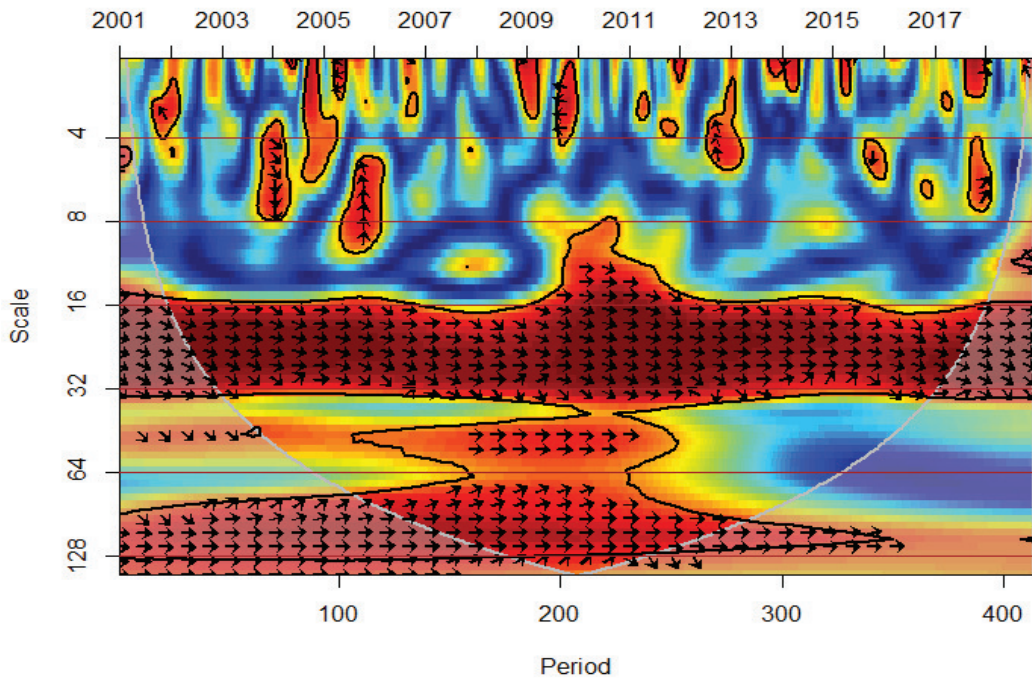
Source: Author's own

Figure 18. The coherence between EVI of the Dense Cerrado and rainfall wavelets.



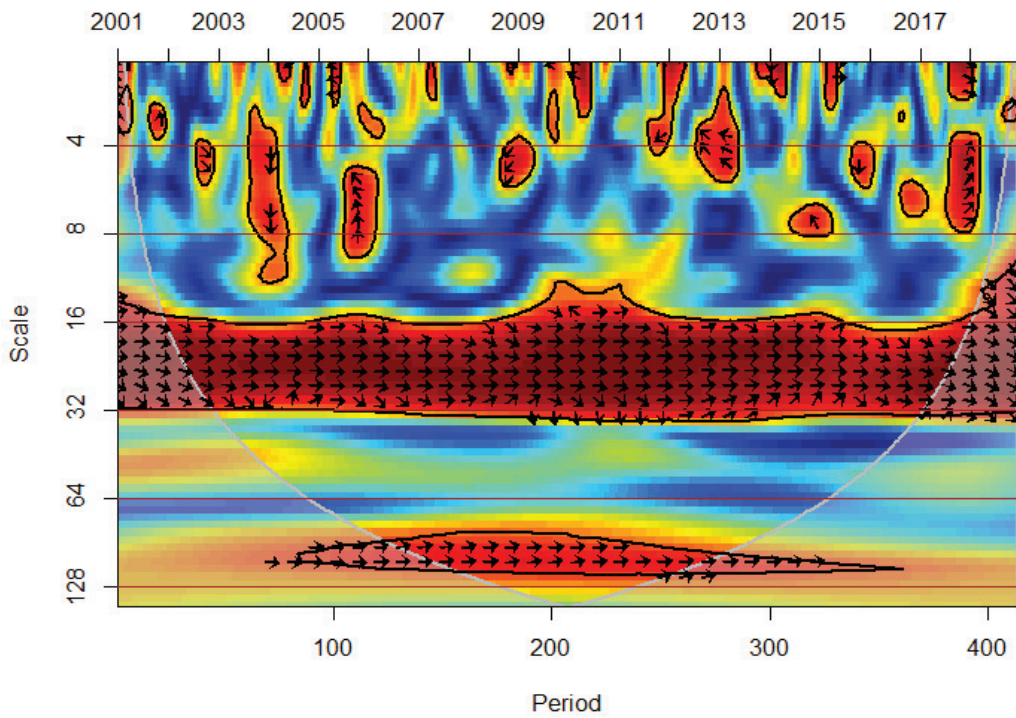
Source: Author's own

Figure 19. The coherence between EVI of the *Cerradão* forest and rainfall wavelets.



Source: Author's own

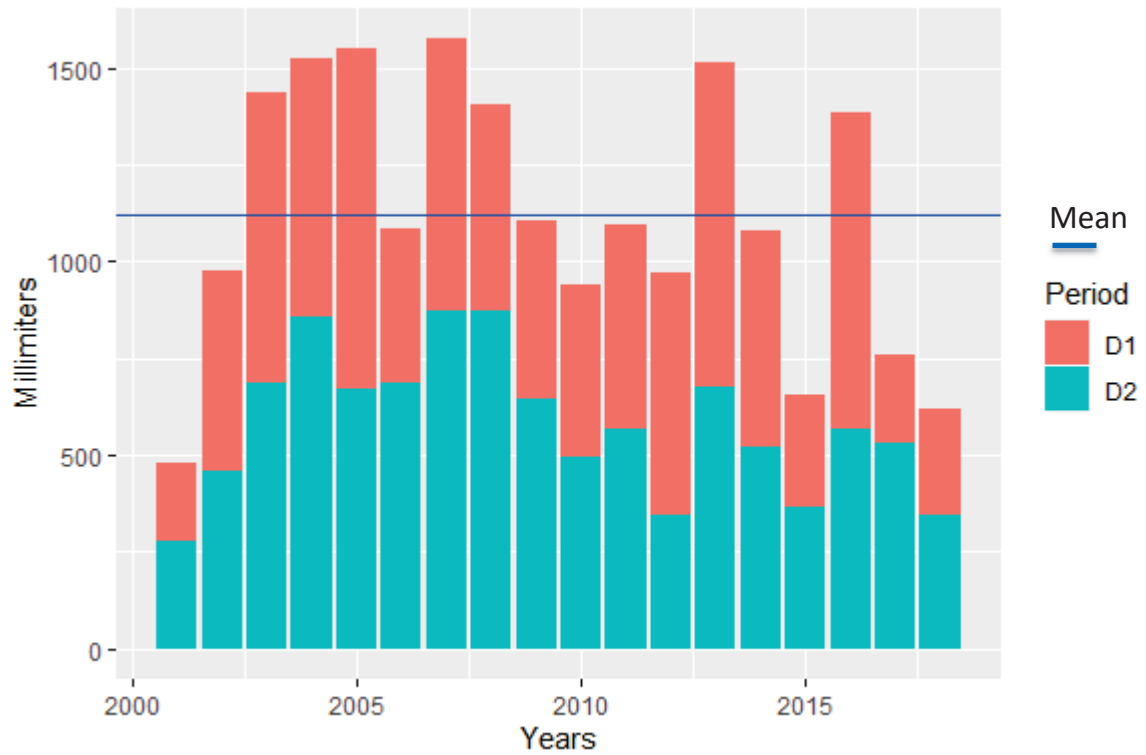
Figure 20. The coherence between EVI of the Seasonal Semi-Deciduous forest and rainfall wavelets.



Source: Author's own

Note: On the figures 13-20, the thick black contour represents the 5% significance level against the red noise. The color code for power range, from blue (low power) to red (high power).

Figure 21. Total rainfall amount in the very short and short-run, D1 (32-64 days) and D2 (4 64-128 days) respectively.



Source: Author's own

#### 4. DISCUSSION

The PCA and TIMESAT results indicate that the physiognomies of Cerrado can be differentiated in most cases by the spectral behavior of their phenological metrics using the NDVI and EVI indices, i.e. they are different in terms of green biomass production over time. The base value, defined as the average of the left and right minimum VI values, and the maximum value, defined as the maximum fitted VI for the growing season values (Jönsson; Eklundh, 2004), revealed a clear gradient for both indices from savanna to forest physiognomies. It can be related to less above-ground biomass in the sparse landscape formations such as TC, which naturally increases with denser vegetation physiognomies (DE MIRANDA *et al.*, 2014). Highest values can be observed for CE and SSF which can consist of up to 15 and 25 m tall trees with crown covers of around 90 and 95% respectively (RIBEIRO; WALTER, 2008). From the spectral response point of view, this pattern happens because as more complex is the canopy (i.e., the higher amount of healthy leaf layers) as higher is the NDVI and EVI value.

The lowest values of growth rate related to greening-up and senescence rate related to browning-down rate for NDVI (Figures 9A - 10A) was observed for SSF. Similar results were found by Schwieder *et al.*, (2016) in the Brazilian Cerrado in center of Brazil where denser vegetation had lowest senescence rate. The vegetation green-up and brown-down behavior can be related to the lower amplitude values (Figures 11A) of this physiognomy and show the buffering effect of the woody vegetation to the dynamic dry–wet cycles of the Cerrado biome (RATANA; HUETE, 2005).

The values of total productivity metric (Figure 12) also follow the savanna to forest gradient with TC presenting the lowest value and SSF with the highest. Modeling radiation absorption as a feature of the fraction of photosynthesis-active radiation absorbed by the canopy (fPAR), which in effect depends on the structure and the canopy's Leaf Area Index (LAI) has been the typical method for calculating whole-canopy photosynthesis and hence Gross Primary Production – GPP. (DAWSON *et al.*, 2003). As known, NDVI and EVI are intrinsically related to chlorophyll and leaf area respectively (HUETE, 1995; ROUSE 1973, 1974), and widely used to determine GPP ((DANELICHEN *et al.*, 2015; SKINNER; WYLIE; GILMANOV, 2011)). The forests' GPP is particularly important because their ability to absorb atmospheric CO<sub>2</sub> plays a significant role in the global carbon cycle (COX *et al.*, 2000).

Together with other seasonal regions in the southern hemisphere (e.g. southern Africa), tropical Brazilian savanna or Cerrado is a seasonal carbon sink during the period of active photosynthesis (FULLER, 1996; GRACE, 2006). Recently, increased atmospheric CO<sub>2</sub> concentrations were suggested to increase the growth rate of trees relative to grasses in savannah areas (DEVINE, 2017; STEVENS, 2017). Also, CO<sub>2</sub> concentration increases have shown to be related to an increase in woody vegetation in savannah areas (ZHANG *et al.*, 2019a).

According to the results found, rainfall is correlated with vegetation indices NDVI and EVI and the coherence of these correlations follows a certain pattern for all Cerrado typologies; the exception is for the SSF EVI coherence where, besides is observed a strong correlation in the middle-run D3 (128-256 days) and D4 (256-512 days), there is no leading phase. The general patterns of correlation and coherence observed for all other results follow:

The short-run D1(32-64 days) and D2 (64-128 days), mainly in the 2004 and 2013, show isolate coherence zones and anomalies in wavelet transformation for rainfall and the most of Cerrado physiognomies for both indices, also the amount of rainfall for the short-run on this period is very higher than average compared to other years, this reveals that intermittent and anomalous, extreme events of rainfall can influence the Cerrado vegetation response. The same pattern has been observed for other semi-arid and arid regions (BAUDENA, 2007, 2008; CHEN, 2020; CHENG, 2011).

The high coherence between the vegetation indexes and rainfall, and the leading phase where vegetation leads precipitation suggests that phenological processes can influence rainfall events in the Brazilian Cerrado in cycles of 8.5 months to 1,5 years, which coincides with the plants growing season and the wet season. It is well known that rainfall events can influence and cause vegetation phenological responses regarding an increase in the productivity in savanna vegetation (BAUDENA 2007; CHEN, 2020; CHENG, 2011). However, the opposite observation of correlation, when vegetation productivity process can be a cause of rainfall events, has been observed most, in areas covered by denser vegetation as in the Amazon basin (SPRACKLEN, 2012; WRIGHT, 2017). Further analyses that include climatological features should be done to confirm the findings presented, but the results showed in this study can pave the way for future researches towards to investigate the possible impact of Cerrado vegetation activity on local, and regional seasonal rainfall events.

The long-run (D5 and D6), also shows a strong coherence, which all rainfall appears leading the coherence over Cerrado physiognomies, and mainly on the savanna-type vegetation. The rainfall wavelet transformation S6 (>128/ 16-days cycles) periods longer



than 2048 days (or 5.7 years) shows a decrease in rainfall in the study area (APPENDIX 1), these findings agree with those results already shown by the Intergovernmental Panel on Climate Change – IPCC, which expect a decrease in rainfall intensity for South America for the next years (KRINNER *et al.*, 2013). On the other hand, it is expected an increase in the frequency of heavy rainfall episodes and droughts, which could favor woody vegetation establishment in these areas (KRINNER, 2013; MASON, 2001). Thus, the intrinsic correlation and coherence between vegetation phenology and rainfall here found shows how savannas and forests of the Cerrado biome are susceptible to climate change.

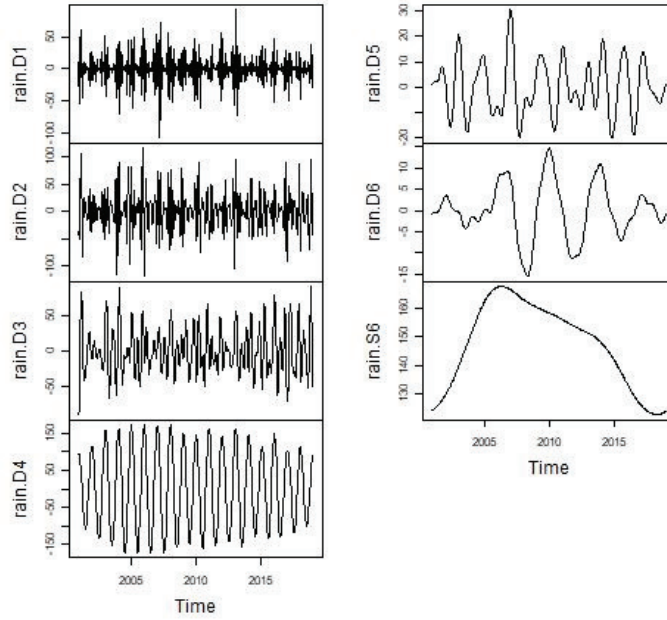
## 5. CONCLUSION

This study has given some insights on the Brazilian savanna phenological behavior and about the connections between rainfall and vegetation types' biophysical response along seventeen years. Cerrado typologies present different spectral-temporal behavior, showing two distinct patterns, one produced by savanna-like physiognomies and other by forest-like physiognomies. We observe that forest physiognomies are more productive seasonally compared to savanna-like vegetation and, thus, the former seems to have a critical role in terms of carbon up-taken across the biome.

There is a strong seasonal relationship between rainfall and physiognomies' biophysical response, and extreme events and long-term trends of rainfall also show coherence with vegetation, showing that climate change impacts the green biomass productivity of various Cerrado biome typologies.

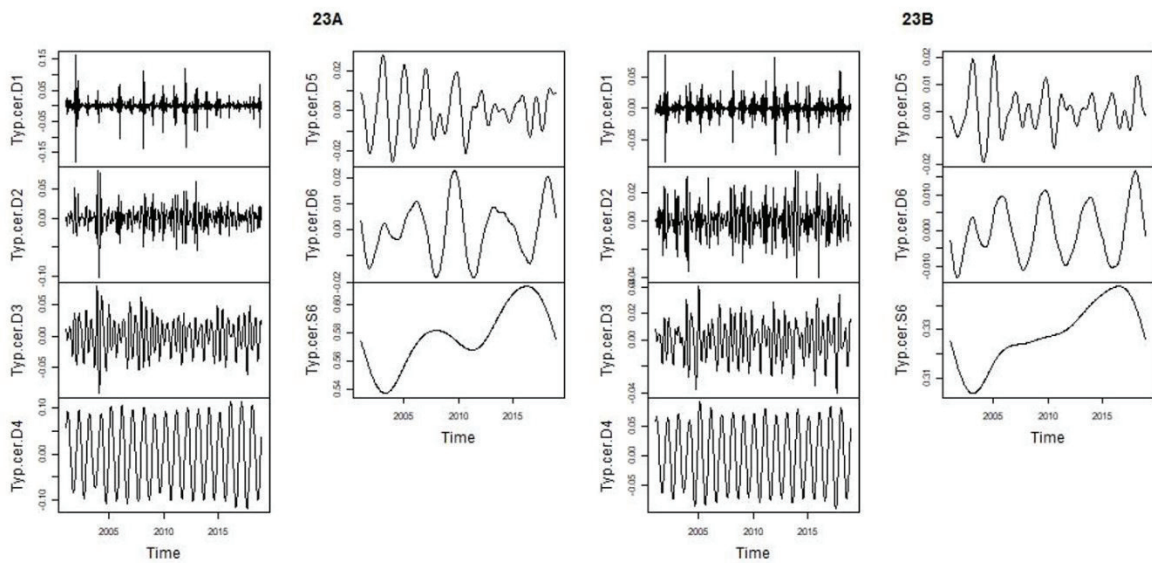
APPENDIX 1 – Wavelet transformation

Figure 22. Rainfall wavelet transformation.



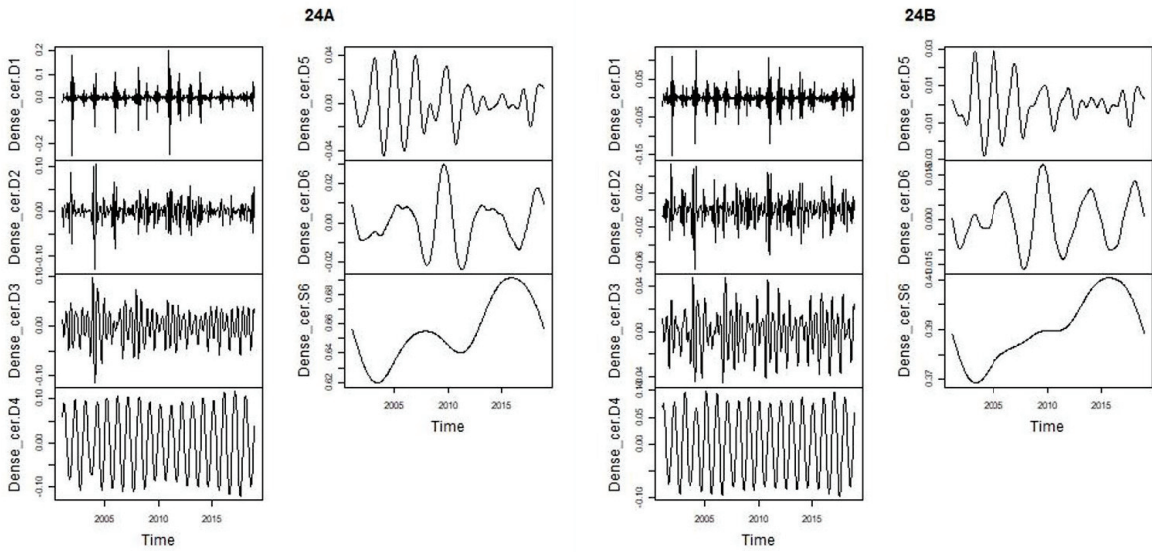
Source: Author's own

Figure 23. Typical Cerrado wavelet transformation (23A – NDVI and 23B – EVI).



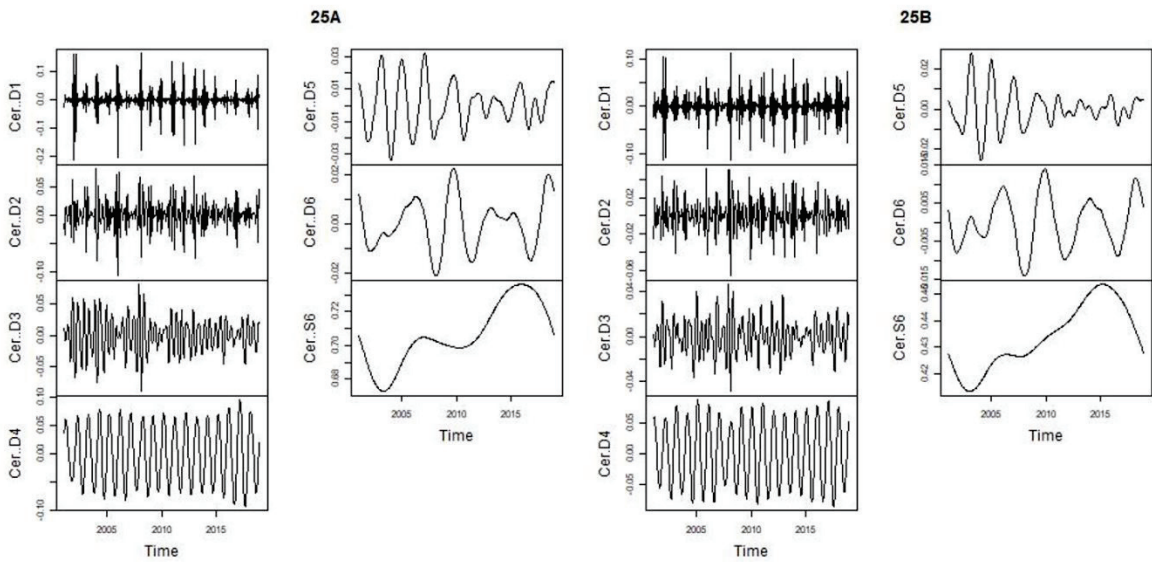
Source: Author's own

Figure 24. Dense Cerrado wavelet transformation (24A – NDVI and 24B – EVI).



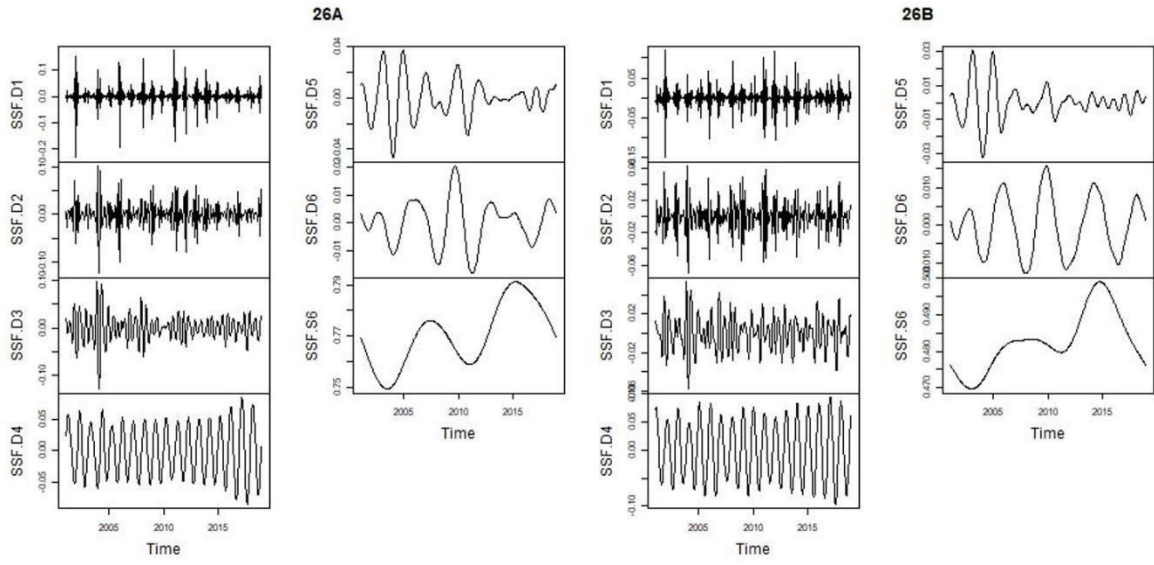
Source: Author's own

Figure 25. Cerradão wavelet transformation (25A – NDVI and 25B – EVI).



Source: Author's own

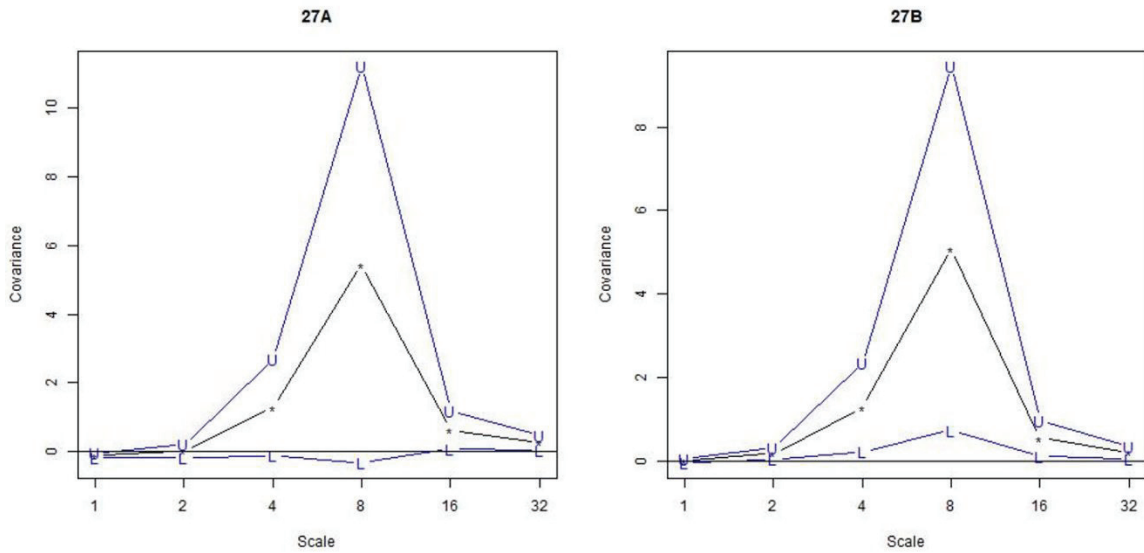
Figure 26. Seasonal Semideciduous Forest (26A – NDVI and 26B – EVI).



Source: Author's own

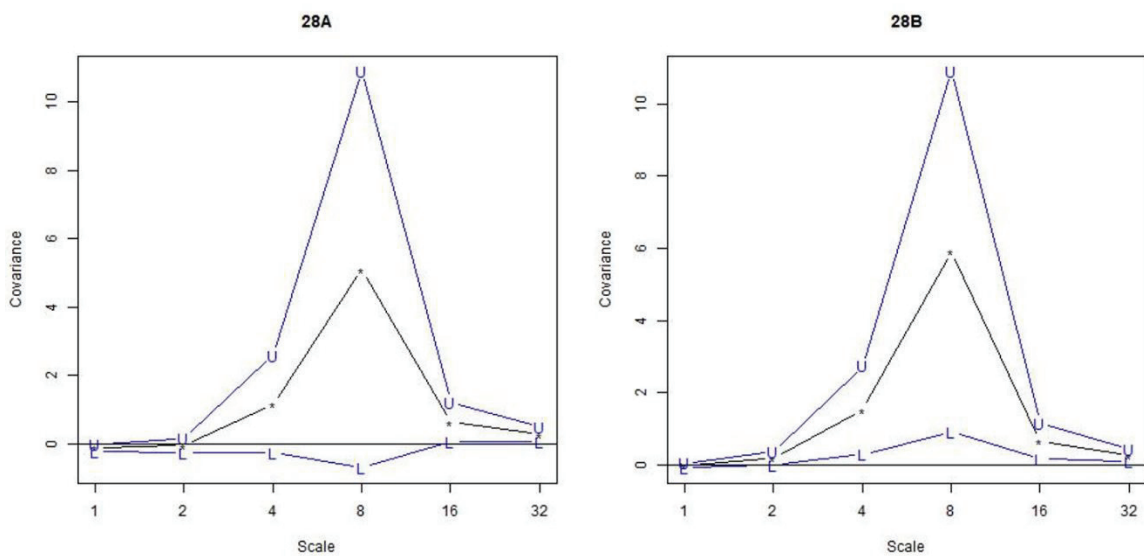
APPENDIX 2 – Covariance among vegetation indices and rainfall.

Figure 27. Covariance among vegetation indices (27A – NDVI and 27B – EVI) and rainfall, for Typical Cerrado.



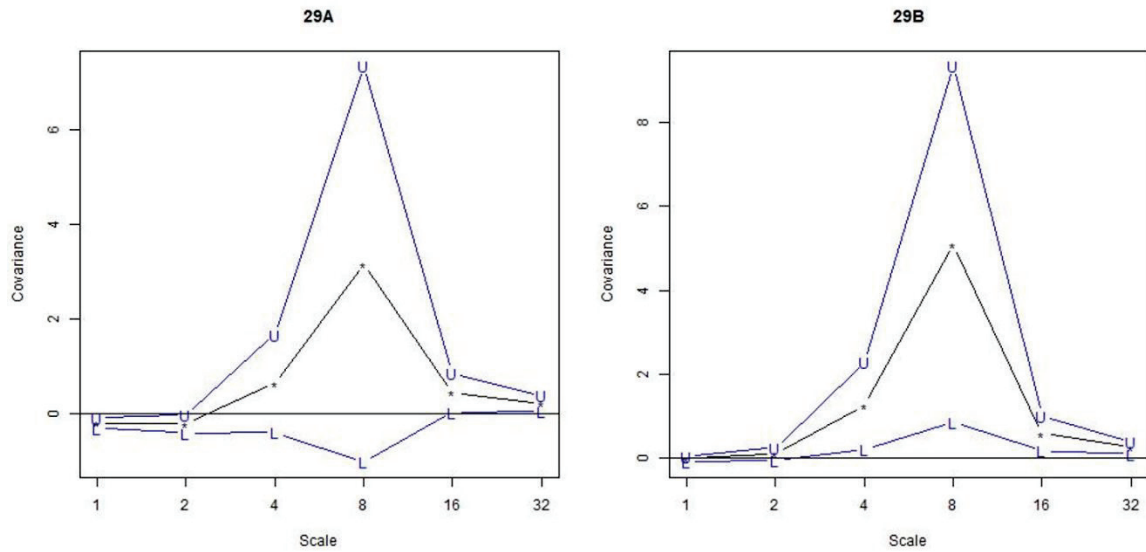
Source: Author's own

Figure 28. Covariance among vegetation indices (28A – NDVI and 28B – EVI) and rainfall, for Dense Cerrado.



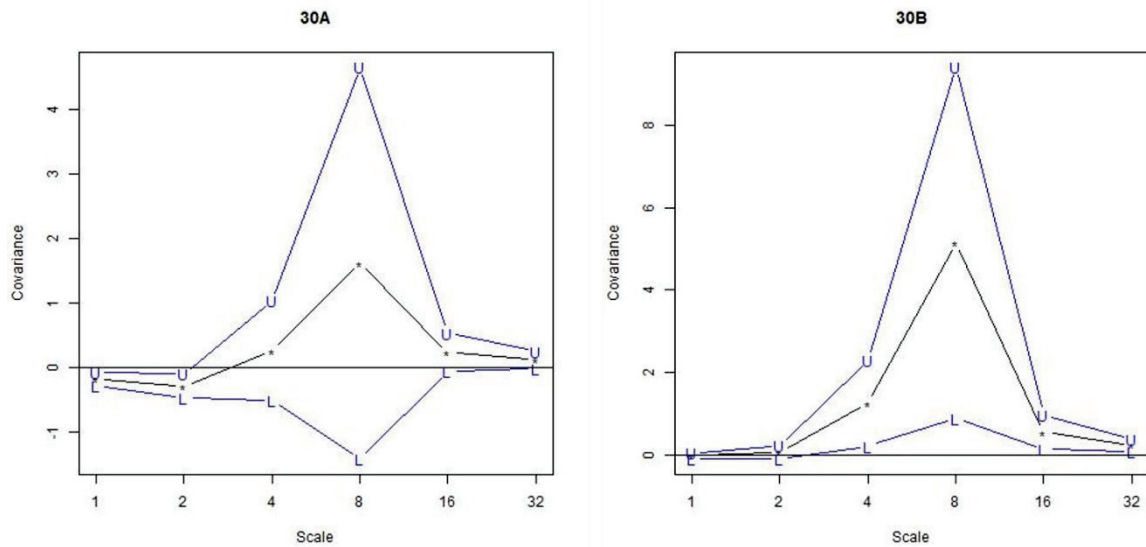
Source: Author's own

Figure 29. Covariance among vegetation indices (29A – NDVI and 29B – EVI) and rainfall, for *Cerradão*.



Source: Author's own

Figure 30. Covariance among vegetation indices (30A – NDVI and 30B – EVI) and rainfall, for Seasonal Semideciduous Forest.

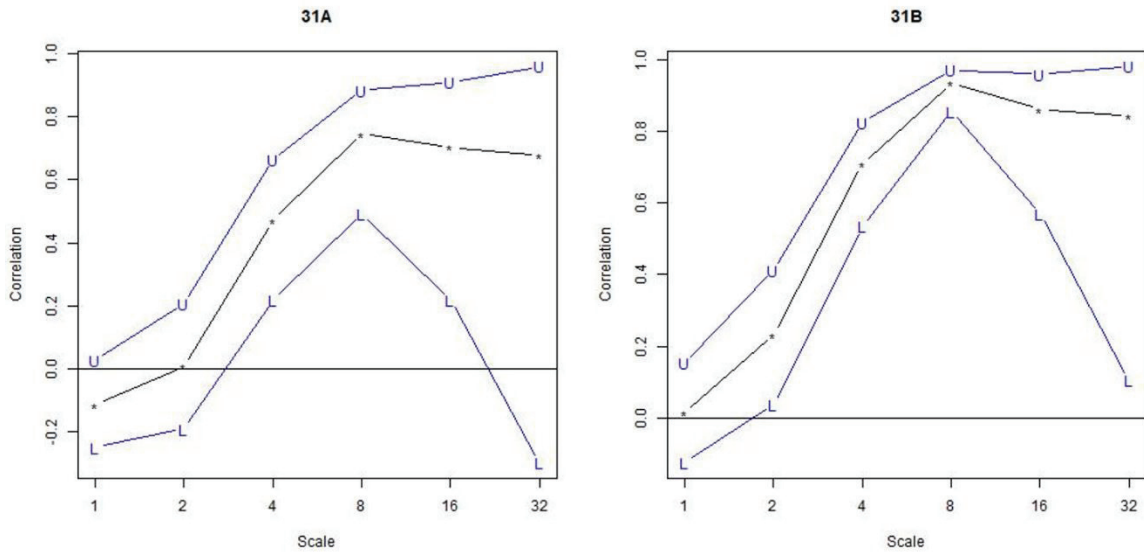


Source: Author's own

Note: The upper and lower bound are represented with “U” and “L” respectively at 95% confidence interval. The black dotted line represents the covariance and correlation among NDVI and EVI of physiognomies and rainfall.

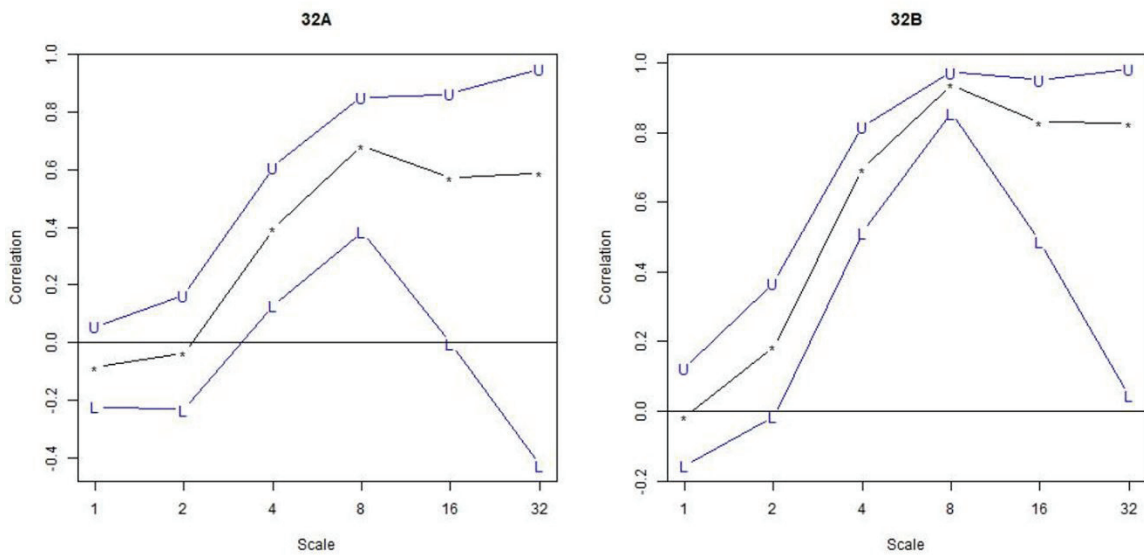
APPENDIX 3 – Correlation among vegetation indices and rainfall.

Figure 31. Correlation among vegetation indices (31A – NDVI and 31B – EVI) and rainfall, for Typical Cerrado.



Source: Author's own

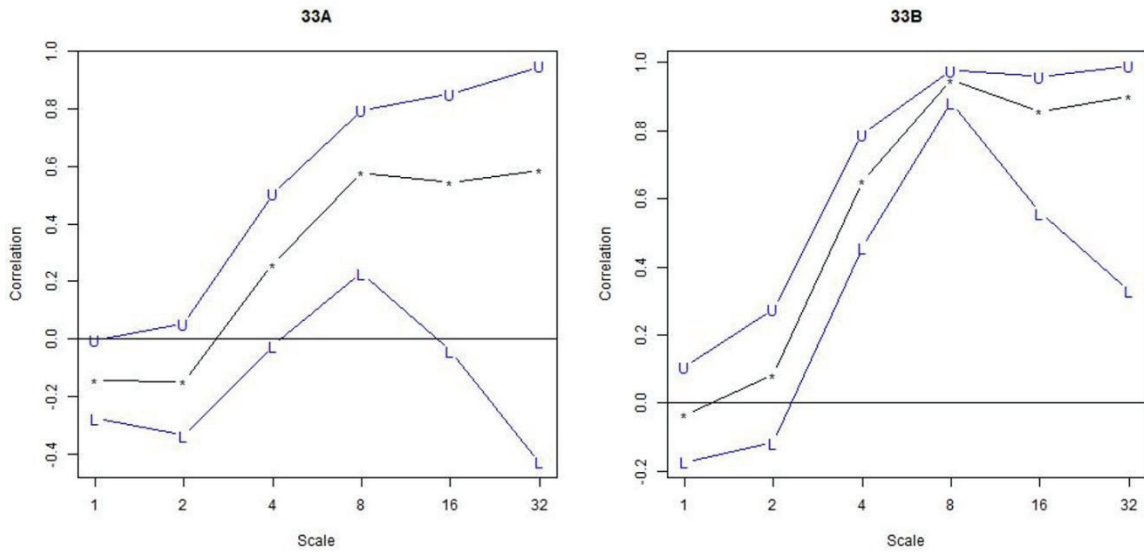
Figure 32. Correlation among vegetation indices (32A – NDVI and 32B – EVI) and rainfall, for Dense Cerrado.



Source: Author's own

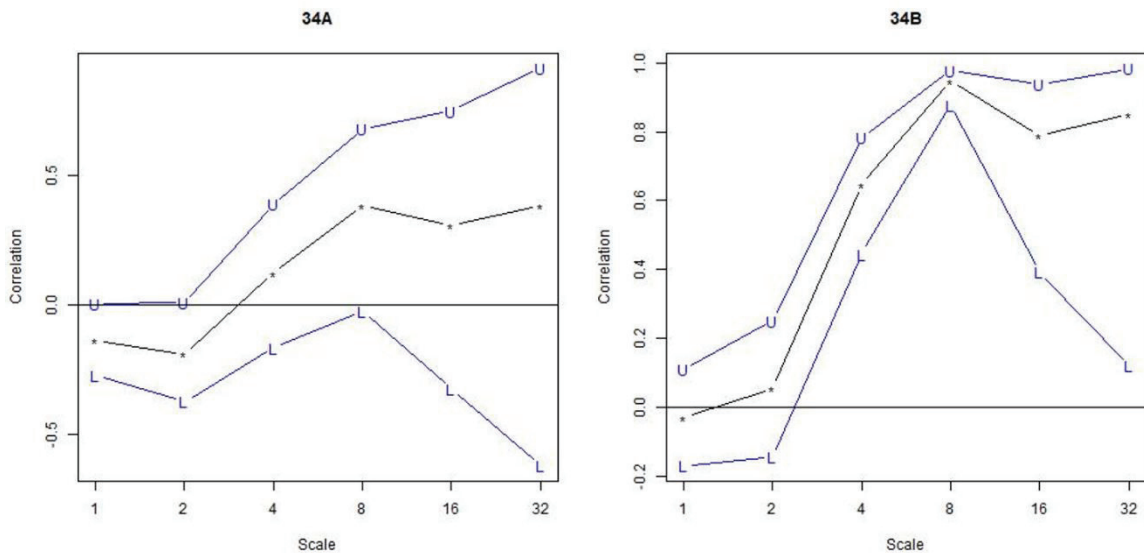


Figure 33. Correlation among vegetation indices (33A – NDVI and 33B – EVI) and rainfall, for *Cerradão*.



Source: Author's own

Figure 34. Correlation among vegetation indices (34A – NDVI and 34B – EVI) and rainfall, for Seasonal Semideciduous Forest.



Source: Author's own

Note: The upper and lower bound are represented with “U” and “L” respectively at 95% confidence interval. The black dotted line represents the covariance and correlation among NDVI and EVI of physiognomies and rainfall.

## 6. REFERENCE

- ALBUQUERQUE, Ana Christina Sagebin; SILVA, Aliomar Gabriel da. **Agricultura Tropical - Quatro décadas de inovações tecnológicas, institucionais e políticas**. [S. l.: s. n.]. *E-book*.
- ANTIQUERA, Lia Maris Orth Ritter; KAGEYAMA, Paulo Yoshio. Genetic diversity of four populations of *Qualea grandiflora* Mart. in fragments of the Brazilian Cerrado. **Genética**, [S. l.], v. 142, n. 1, p. 11–21, 2014. Disponível em: <https://doi.org/10.1007/s10709-013-9750-5>
- ASNER, Gregory P.; MARTIN, Roberta E. Canopy phylogenetic, chemical and spectral assembly in a lowland Amazonian forest. **New Phytologist**, [S. l.], v. 189, n. 4, p. 999–1012, 2011. Disponível em: <https://doi.org/10.1111/j.1469-8137.2010.03549.x>
- BALDUINO, Alexander Paulo do Carmo *et al.* Fitossociologia e análise comparativa da composição florística do cerrado da flora de Paraopeba-MG. **Revista Árvore**, [S. l.], v. 29, n. 1, p. 25–34, 2006. Disponível em: <https://doi.org/10.1590/s0100-67622005000100004>
- BAUDENA, M. *et al.* Vegetation response to rainfall intermittency in drylands: Results from a simple ecohydrological box model. **Advances in Water Resources**, [S. l.], v. 30, n. 5, p. 1320–1328, 2007. Disponível em: <https://doi.org/10.1016/j.advwatres.2006.11.006>
- BAUDENA, M.; PROVENZALE, A. Rainfall intermittency and vegetation feedbacks in drylands. **Hydrology and Earth System Sciences**, [S. l.], v. 12, n. 2, p. 679–689, 2008. Disponível em: <https://doi.org/10.5194/hess-12-679-2008>
- BELLIER, Edwige *et al.* D. Borcard, F. Gillet, P. Legendre: Numerical Ecology with R. **Journal of Agricultural, Biological, and Environmental Statistics**, [S. l.], v. 17, n. 2, p. 308–309, 2012. Disponível em: <https://doi.org/10.1007/s13253-012-0094-x>
- BOELMAN, Natalie T. *et al.* Inter-annual variability of NDVI in response to long-term warming and fertilization in wet sedge and tussock tundra. **Oecologia**, [S. l.], v. 143, n. 4, p. 588–597, 2005. Disponível em: <https://doi.org/10.1007/s00442-005-0012-9>
- BURKE-HUBBARD, B. **The World According to Wavelets. The story of a Mathematical Technique in the Making**. 2. ed. Natick, Massachusetts: A.K. Peters, 1998. *E-book*.
- BUSETTO, Lorenzo; RANGHETTI, Luigi. MODISstsp: A Tool for Automatic Preprocessing of. **Computers & Geosciences**, [S. l.], v. 97, p. 40–48, 2016. Disponível em: <https://github.com/ropensci/MODISstsp>
- BUSTAMANTE, MMC *et al.* Potential impacts of climate change on biogeochemical functioning of Cerrado ecosystems. **Brazilian Journal of Biology**, [S. l.], v. 72, n. 3 suppl, p. 655–671, 2012. Disponível em: <https://doi.org/10.1590/s1519-69842012000400005>
- CAMARGO, Maria Gabriela Gutierrez *et al.* Effects of environmental conditions associated to the cardinal orientation on the reproductive phenology of the cerrado savanna tree *Xylopia aromatica* (Annonaceae). **Anais da Academia Brasileira de Ciências**, [S. l.], v. 83, n. 3, p. 1007–1019, 2011. Disponível em: <https://doi.org/10.1590/S0001-37652011005000014>
- CHEN, Zefeng; WANG, Weiguang; FU, Jianyu. Vegetation response to precipitation anomalies under different climatic and biogeographical conditions in China. **Scientific**

**Reports**, [S. l.], v. 10, n. 1, p. 1–16, 2020. Disponível em: <https://doi.org/10.1038/s41598-020-57910-1>

CHENG, Y. *et al.* Impact of rainfall variability and grazing pressure on plant diversity in Mongolian grasslands. **Journal of Arid Environments**, [S. l.], v. 75, n. 5, p. 471–476, 2011. Disponível em: <https://doi.org/10.1016/j.jaridenv.2010.12.019>

CHOUAKRI, S. A. Wavelet Analysis Versus Fourier Analysis : Application To Time-Varying Spectra Signals WAVELET ANALYSIS VERSUS FOURIER ANALYSIS : APPLICATION TO TIME-VARYING SPECTRA SIGNALS. [S. l.], n. October, 2016.

COOGAN, Sean C. P. *et al.* Scientists' warning on wildfire — a canadian perspective. **Canadian Journal of Forest Research**, [S. l.], v. 49, n. 9, p. 1015–1023, 2019. Disponível em: <https://doi.org/10.1139/cjfr-2019-0094>

COUTINHO, L. M. Fire in the Ecology of the Brazilian Cerrado. [S. l.], p. 82–105, 1990. Disponível em: [https://doi.org/10.1007/978-3-642-75395-4\\_6](https://doi.org/10.1007/978-3-642-75395-4_6)

COX, Peter M. *et al.* Acceleration of global warming due to carbon-cycle feedbacks in a coupled climate model. **Nature**, [S. l.], 2000. Disponível em: <https://doi.org/10.1038/35041539>

DA SILVA, Fernando Macena *et al.* Clima do Bioma Cerrado. *In: Agricultura Tropical: Quatro décadas de inovações tecnológicas, institucionais e políticas.* [S. l.: s. n.]. p. 93–148. *E-book.*

DANELICHEN, Victor H. M. *et al.* Estimating of gross primary production in an Amazon-cerrado transitional forest using MODIS and landsat imagery. **Anais da Academia Brasileira de Ciências**, [S. l.], v. 87, n. 3, p. 1545–1564, 2015. Disponível em: <https://doi.org/10.1590/0001-3765201520140457>

DAWSON, T. P. *et al.* Forest ecosystem chlorophyll content: Implications for remotely sensed estimates of net primary productivity. **International Journal of Remote Sensing**, [S. l.], v. 24, n. 3, p. 611–617, 2003. Disponível em: <https://doi.org/10.1080/01431160304984>

DE ALMEIDA, Teodoro Isnard Ribeiro *et al.* Principal component analysis applied to a time series of MODIS images: the spatio-temporal variability of the Pantanal wetland, Brazil. **Wetlands Ecology and Management**, [S. l.], v. 23, n. 4, p. 737–748, 2015. Disponível em: <https://doi.org/10.1007/s11273-015-9416-4>

DE BEURS, K. M.; HENEERY, G. M. A statistical framework for the analysis of long image time series. **International Journal of Remote Sensing**, [S. l.], v. 26, n. 8, p. 1551–1573, 2005. Disponível em: <https://doi.org/10.1080/01431160512331326657>

DE MATTOS, Eduardo A.; LOBO, Patrícia C.; JOLY, Carlos A. Overnight rainfall inducing rapid changes in photosynthetic behaviour in a cerrado woody species during a dry spell amidst the rainy season. **Australian Journal of Botany**, [S. l.], v. 50, n. 2, p. 241–246, 2002. Disponível em: <https://doi.org/10.1071/BT01023>

DE MIRANDA, Sabrina do Couto *et al.* Regional variations in biomass distribution in Brazilian Savanna Woodland. **Biotropica**, [S. l.], v. 46, n. 2, p. 125–138, 2014. Disponível em: <https://doi.org/10.1111/btp.12095>

DEVINE, Aisling P. *et al.* Determinants of woody encroachment and cover in African

savannas. **Oecologia**, [S. l.], v. 183, n. 4, p. 939–951, 2017. Disponível em: <https://doi.org/10.1007/s00442-017-3807-6>

DIDAN, Kamel; MUNOZ, Armando Barreto; HUETE, Alfredo. **MODIS Vegetation Index User's Guide**. Tucson: [s. n.], 2015. Disponível em: [http://modis-sr.ltdri.org/guide/MOD09\\_UserGuide\\_v1.4.pdf](http://modis-sr.ltdri.org/guide/MOD09_UserGuide_v1.4.pdf)

DING, Mingjun *et al.* The relationship between NDVI and precipitation on the Tibetan Plateau. **Journal of Geographical Sciences**, [S. l.], v. 17, n. 3, p. 259–268, 2007. Disponível em: <https://doi.org/10.1007/s11442-007-0259-7>

EITEN, George. The cerrado vegetation of Brazil. **The New York Botanical Garden**, [S. l.], v. 38, n. 2, p. 201–341, 1972. Disponível em: [www.jstor.org/stable/4353829](http://www.jstor.org/stable/4353829)

ELTHAIR, E. A. B.; BRAS, R. L. Precipitation recycling in the Amazon basin. **Q. J. R. Meteorol. Soc.**, [S. l.], v. 1, n. 120, p. 861–880, 1994.

ENCINAS, José Imaña; MACEDO, Lucélia Alves; PAULA, José Elias. FLORÍSTICA E FITOSSOCIOLOGIA DE UM TRECHO DA FLORESTA ESTACIONAL SEMIDECIDUAL NA ÁREA DO ECOMUSEU DO CERRADO, EM PIRENÓPOLIS GOIÁS. **CERNE**, [S. l.], v. 13, p. 308–320, 2007.

ESRI. **ArcGIS Desktop: Release 10.2**. [S. l.: s. n.]

FELFILI, Jeanine Maria; CARVALHO, Fabrício Alvim; HAIDAR, Ricardo Flores. Manual para o monitoramento de parcelas permanentes nos biomas Cerrado e Pantanal. **Universidade de Brasília Departamento de Engenharia Florestal**, [S. l.], v. 54, n. February 2015, p. 51, 2005.

FILHO, E. F. **Collection of functions to fit models with emphasis in land use and soil mapping**. [S. l.: s. n.]

FULLER, Douglas O.; PRINCE, Stephen D. Rainfall and foliar dynamics in tropical southern Africa: Potential impacts of global climatic change on Savanna vegetation. **Climatic Change**, [S. l.], v. 33, n. 1, p. 69–96, 1996. Disponível em: <https://doi.org/10.1007/BF00140514>

GALLEGATI, Marco *et al.* **The US Wage Phillips Curve across Frequencies and over Time**. [S. l.: s. n.] Disponível em: <https://doi.org/10.1111/j.1468-0084.2010.00624.x>

GESSNER, Ursula *et al.* The relationship between precipitation anomalies and satellite-derived vegetation activity in Central Asia. **Global and Planetary Change**, [S. l.], v. 110, p. 74–87, 2013. Disponível em: <https://doi.org/10.1016/j.gloplacha.2012.09.007>

GRACE, John *et al.* Productivity and carbon fluxes of tropical savannas. **Journal of Biogeography**, [S. l.], v. 33, n. 3, p. 387–400, 2006. Disponível em: <https://doi.org/10.1111/j.1365-2699.2005.01448.x>

GRAMATIKOV, B.; GEORGIEV, I. Wavelets as alternative to short-time Fourier transform in signal-averaged electrocardiography. **Medical & Biological Engineering & Computing**, [S. l.], v. 33, n. 3, p. 482–487, 1995. Disponível em: <https://doi.org/10.1007/BF02510534>

GRAPS, Amara. An Introduction to Wavelets. **IEEE Computational Science and Engineering**, [S. l.], v. 2, p. 1–18, 1995.

GRECCHI, Rosana Cristina *et al.* Land use and land cover changes in the Brazilian Cerrado: A multidisciplinary approach to assess the impacts of agricultural expansion. **Applied Geography**, [S. l.], v. 55, p. 300–312, 2014. Disponível em: <https://doi.org/10.1016/j.apgeog.2014.09.014>

HUETE, A. *et al.* Overview of the radiometric and biophysical performance of the MODIS vegetation indices. **Remote Sensing of Environment**, [S. l.], v. 83, p. 195–213, 2002.

HUETE, A. R. *et al.* A Comparison of Vegetation Indices over a Global Set of TM Images for EOS-MODIS. [S. l.], v. 4257, n. Table 1, 1995.

JIANG, Zhangyan *et al.* Development of a two-band enhanced vegetation index without a blue band. **Remote Sensing of Environment**, [S. l.], v. 112, n. 10, p. 3833–3845, 2008. Disponível em: <https://doi.org/10.1016/j.rse.2008.06.006>

JÖNSSON, Per; EKLUNDH, Lars. TIMESAT — a program for analyzing time-series of satellite sensor data \$. **Computers & Geosciences**, [S. l.], v. 30, p. 833–845, 2004. Disponível em: <https://doi.org/10.1016/j.cageo.2004.05.006>

JUSTICE, C. O. *et al.* An overview of MODIS Land data processing and product status. **Remote Sensing of Environment**, [S. l.], v. 83, n. 1–2, p. 3–15, 2002. Disponível em: [https://doi.org/10.1016/S0034-4257\(02\)00084-6](https://doi.org/10.1016/S0034-4257(02)00084-6)

KIM, Sangdan. Wavelet Analysis of Precipitation Variability in Northern California, U.S.A. **KSCE Journal of Civil Engineering**, [S. l.], v. 8, n. 4, p. 471–477, 2004. Disponível em: <http://link.springer.com/content/pdf/10.1007%2FBF02829169.pdf%5Cnfile:///Users/vaniarosa/Documents/Papers/Unknown/Unknown/Untitled-p2767.pdf%5Cnpapers://d28dd570-4187-41d3-8cf5-6edf67fea1b9/Paper/p2767>

KLINK, Carlos A.; MACHADO, Ricardo B. Conservation of the Brazilian Cerrado. **Conservation Biology**, [S. l.], v. 19, n. 3, p. 707–713, 2005.

KRINNER, Gerhard *et al.* Long-term climate change: Projections, commitments and irreversibility. **Climate Change 2013 the Physical Science Basis: Working Group I Contribution to the Fifth Assessment Report of the Intergovernmental Panel on Climate Change**, [S. l.], v. 9781107057, p. 1029–1136, 2013. Disponível em: <https://doi.org/10.1017/CBO9781107415324.024>

LABAT, David; ABABOU, R.; MANGIN, A. Rainfall-runoff relations for karstic springs. Part II: Continuous wavelet and discrete orthogonal multiresolution analyses. **Journal of Hydrology**, [S. l.], v. 238, n. 3–4, p. 149–178, 2000. Disponível em: [https://doi.org/10.1016/S0022-1694\(00\)00322-X](https://doi.org/10.1016/S0022-1694(00)00322-X)

LIETH, Helmut. Purposes of a Phenology Book. *In: [S. l.: s. n.]. E-book.* Disponível em: [https://doi.org/10.1007/978-3-642-51863-8\\_1](https://doi.org/10.1007/978-3-642-51863-8_1)

LOO, Yen Yi; BILLA, Lawal; SINGH, Ajit. Effect of climate change on seasonal monsoon in Asia and its impact on the variability of monsoon rainfall in Southeast Asia. **Geoscience Frontiers**, [S. l.], v. 6, n. 6, p. 817–823, 2015. Disponível em: <https://doi.org/10.1016/j.gsf.2014.02.009>

MALLAT, Stephane G. A theory for multiresolution signal decomposition: The wavelet representation. **Fundamental Papers in Wavelet Theory**, [S. l.], v. II, n. 7, p. 494–513, 2009. Disponível em: <https://doi.org/10.1515/9781400827268.494>

MARTÍNEZ, Beatriz; GILABERT, María Amparo. Vegetation dynamics from NDVI time series analysis using the wavelet transform. **Remote Sensing of Environment**, [S. l.], v. 113, n. 9, p. 1823–1842, 2009. Disponível em: <https://doi.org/10.1016/j.rse.2009.04.016>

MASON, Simon J.; GODDARD, Lisa. Probabilistic precipitation anomalies associated with ENSO. **Bulletin of the American Meteorological Society**, [S. l.], v. 82, n. 4, p. 619–638, 2001. Disponível em: [https://doi.org/10.1175/1520-0477\(2001\)082<0619:PPAAWE>2.3.CO;2](https://doi.org/10.1175/1520-0477(2001)082<0619:PPAAWE>2.3.CO;2)

MENENTI, M. *et al.* Mapping agroecological zones and time lag in vegetation growth by means of fourier analysis of time series of NDVI images. **Advances in Space Research**, [S. l.], v. 13, n. 5, p. 233–237, 1993. Disponível em: [https://doi.org/10.1016/0273-1177\(93\)90550-U](https://doi.org/10.1016/0273-1177(93)90550-U)

MUELLER, Lothar *et al.* Above ground biomass and water use efficiency of crops at shallow water tables in a temperate climate. **Agricultural Water Management**, [S. l.], v. 75, n. 2, p. 117–136, 2005. Disponível em: <https://doi.org/10.1016/j.agwat.2004.12.006>

MYERS, Norman *et al.* Biodiversity hotspots for conservation priorities. **Nature**, [S. l.], v. 403, p. 853–858, 2000. Disponível em: <https://doi.org/10.1038/35002501>

NASI, Robert *et al.* Forest fire and biological diversity. **Unasylva**, [S. l.], 2002.

NEUPAUER, Roseanna M. *et al.* Characterization of permeability anisotropy using wavelet analysis. **Water Resources Research**, [S. l.], v. 42, n. 7, p. 1–13, 2006. Disponível em: <https://doi.org/10.1029/2005WR004364>

OKSANEN, Jari *et al.* **vegan: Community Ecology Package. R package version 2.5-6.** [S. l.: s. n.] Disponível em: <https://cran.r-project.org/package=vegan%0A>

PERCIVAL, D. B.; WANG, M.; OVERLAND, J. E. An introduction to wavelet analysis with applications to vegetation time series. **Community Ecology**, [S. l.], v. 5, n. 1, p. 19–30, 2004. Disponível em: <https://doi.org/10.1556/ComEc.5.2004.1.3>

PERCIVAL DONALD. On Estimation of the wavelet variance. **Biometrika**, [S. l.], v. 82, n. 3, p. 619–631, 1995. Disponível em: <https://doi.org/10.1214/aoms/1177698699>

PIAO, Shilong *et al.* Variations in satellite-derived phenology in China's temperate vegetation. **Global Change Biology**, [S. l.], v. 12, n. 4, p. 672–685, 2006. Disponível em: <https://doi.org/10.1111/j.1365-2486.2006.01123.x>

QUINTÃO, I. R. **CONSISTÊNCIA DE DADOS SAZONAIS MODERATE RESOLUTION IMAGING SPECTRORADIOMETER (MODIS) NA CARACTERIZAÇÃO DE FITOFISIONOMIAS DO BIOMA CERRADO.** 2018. - Universidade Federal de Viçosa, [s. l.], 2018.

R CORE TEAM. **A Language and Environment for Statistical Computing.** Vienna, Austria: [s. n.], 2018.

RAPINEL, Sébastien *et al.* Mapping the functional dimension of vegetation series in the Mediterranean region using multitemporal MODIS data. **GIScience and Remote Sensing**, [S. l.], v. 00, n. 00, p. 1–14, 2019. Disponível em: <https://doi.org/10.1080/15481603.2019.1662167>

RATANA, Piyachat; HUETE, Alfredo R. Analysis of Cerrado Physiognomies and Conversion in the MODIS Seasonal – Temporal Domain. *[S. l.]*, v. 9, n. 3, 2005.

RATTER, J. A.; RIBEIRO, J. F.; BRIDGEWATER, S. The Brazilian cerrado vegetation and threats to its biodiversity. **Annals of Botany**, *[S. l.]*, v. 80, n. 3, p. 223–230, 1997. Disponível em: <https://doi.org/10.1006/anbo.1997.0469>

RIBEIRO, J. F.; WALTER, Bruno M. T. As principais fitofisionomias do bioma Cerrado. *In: Cerrado: Ecologia e flora*. 2. ed. Brasília: Embrapa Cerrados, 2008. *E-book*. Disponível em: [https://www.researchgate.net/publication/283072910\\_As\\_principais\\_fitofisionomias\\_do\\_bioma\\_Cerrado](https://www.researchgate.net/publication/283072910_As_principais_fitofisionomias_do_bioma_Cerrado)

ROERINK, G. J.; MENENTI, M.; VERHOEF, W. Reconstructing cloudfree NDVI composites using Fourier analysis of time series. **International Journal of Remote Sensing**, *[S. l.]*, v. 21, n. 9, p. 1911–1917, 2000. Disponível em: <https://doi.org/10.1080/014311600209814>

ROSSI, Mattia *et al.* A Comparison of the Signal from Diverse Optical Sensors for Monitoring Alpine Grassland Dynamics. **Remote Sensing**, *[S. l.]*, v. 11, n. 3, p. 296, 2019. Disponível em: <https://doi.org/10.3390/rs11030296>

ROUSE, J. W. *et al.* Monitoring vegetation systems in the great plains with ERTS. **Third Earth Resources Technology Satellite (ERTS) symposium**, *[S. l.]*, v. 1, p. 309–317, 1973. Disponível em: <https://doi.org/citeulike-article-id:12009708>

ROUSE, J. W. *et al.* Monitoring the vernal advancement and retrogradation (green wave effect) of natural vegetation. **Final Report, RSC 1978-4, Texas A & M University, College Station, Texas**, *[S. l.]*, 1974.

SANG, Yan Fang. A review on the applications of wavelet transform in hydrology time series analysis. **Atmospheric Research**, *[S. l.]*, v. 122, p. 8–15, 2013. Disponível em: <https://doi.org/10.1016/j.atmosres.2012.11.003>

SANO, Edson Eyji *et al.* Mapeamento de cobertura vegetal do bioma Cerrado: estratégias e resultados. **Embrapa**, *[S. l.]*, v. 190, p. 33, 2007. Disponível em: <http://www.mendeley.com/research/mapeamento-cobertura-vegetal-bioma-cerrado-estrategias-e-resultados/>

SCHULTZ, P. A.; HALPERT, M. S. Global correlation of temperature, NDVI and precipitation. **Advances in Space Research**, *[S. l.]*, v. 13, n. 5, p. 277–280, 1993. Disponível em: [https://doi.org/10.1016/0273-1177\(93\)90559-T](https://doi.org/10.1016/0273-1177(93)90559-T)

SCHWIEDER, Marcel *et al.* Mapping Brazilian savanna vegetation gradients with Landsat time series. **International Journal of Applied Earth Observation and Geoinformation**, *[S. l.]*, v. 52, p. 361–370, 2016. Disponível em: <https://doi.org/10.1016/j.jag.2016.06.019>

SKINNER, R. H.; WYLIE, B. K.; GILMANOV, T. G. Using normalized difference vegetation index to estimate carbon fluxes from small rotationally grazed pastures. **Agronomy Journal**, *[S. l.]*, v. 103, n. 4, p. 972–979, 2011. Disponível em: <https://doi.org/10.2134/agronj2010.0495>

SPRACKLEN, D. V.; ARNOLD, S. R.; TAYLOR, C. M. Observations of increased tropical rainfall preceded by air passage over forests. **Nature**, *[S. l.]*, v. 489, n. 7415, p. 282–285,

2012. Disponível em: <https://doi.org/10.1038/nature11390>

STEINBUCH, M.; VAN DE MOLENGRAF, TM. J. .. Wavelet theory and its applications. **Choice Reviews Online**, [S. l.], v. 30, n. 09, p. 30-5031-30–5031, 2013. Disponível em: <https://doi.org/10.5860/choice.30-5031>

STEVENS, Nicola *et al.* Savanna woody encroachment is widespread across three continents. **Global Change Biology**, [S. l.], v. 23, n. 1, p. 235–244, 2017. Disponível em: <https://doi.org/10.1111/gcb.13409>

TAIZ, Lincoln; ZEIGER, Eduardo. **Plant Physiology. 3rd edn.** [S. l.: s. n.]. E-book. Disponível em: <https://doi.org/10.1093/aob/mcg079>

WHITCHER, Author Brandon. **waveslim: Basic Wavelet Routines for One-, Two- And Three-Dimensional Signal Processing.** [S. l.: s. n.] Disponível em: <https://cran.r-project.org/package=waveslim>

WHITCHER, Brandon. **waveslim: Basic wavelet routines for one-, two- and three-dimensional signal processing.** [S. l.: s. n.] Disponível em: <http://cran.r-project.org/package=waveslim>

WICKHAM, Hadley; WINSTON, Chang. **Create Elegant Data Visualisations Using the Grammar of Graphics.** [S. l.: s. n.] Disponível em: <https://doi.org/10.1093/bioinformatics/btr406>

WRIGHT, Jonathon S. *et al.* Rainforest-initiated wet season onset over the southern Amazon. **Proceedings of the National Academy of Sciences of the United States of America**, [S. l.], v. 114, n. 32, p. 8481–8486, 2017. Disponível em: <https://doi.org/10.1073/pnas.1621516114>

WYLIE, B. K. *et al.* Satellite mapping of surface biophysical parameters at the biome scale over the North American grasslands a case study. **Remote Sensing of Environment**, [S. l.], v. 79, n. 2–3, p. 266–278, 2002. Disponível em: [https://doi.org/10.1016/S0034-4257\(01\)00278-4](https://doi.org/10.1016/S0034-4257(01)00278-4)

XU, Panpan; NIU, Zhenguang; TANG, Ping. Comparison and assessment of NDVI time series for seasonal wetland classification. **International Journal of Digital Earth**, [S. l.], v. 11, n. 11, p. 1103–1131, 2018. Disponível em: <https://doi.org/10.1080/17538947.2017.1375563>

ZHANG, Wenmin *et al.* rainfall climatology in tropical savannas. **Nature Communications**, [S. l.], 2019 a. Disponível em: <https://doi.org/10.1038/s41467-019-08602-6>

ZHANG, Xiaoyang *et al.* Monitoring vegetation phenology using MODIS. **Remote Sensing of Environment**, [S. l.], v. 84, n. 3, p. 471–475, 2003. Disponível em: [https://doi.org/10.1016/S0034-4257\(02\)00135-9](https://doi.org/10.1016/S0034-4257(02)00135-9)

ZHANG, Xiaoyang *et al.* Monitoring the response of vegetation phenology to precipitation in Africa by coupling MODIS and TRMM instruments. **JOURNAL OF GEOPHYSICAL RESEARCH**, [S. l.], v. 110, p. 1–14, 2005. Disponível em: <https://doi.org/10.1029/2004JD005263>

ZHANG, Yihang *et al.* Mapping annual forest cover by fusing PALSAR/PALSAR-2 and MODIS NDVI during 2007–2016. **Remote Sensing of Environment**, [S. l.], v. 224, n. October 2018, p. 74–91, 2019 b. Disponível em: <https://doi.org/10.1016/j.rse.2019.01.038>